Reports of the Department of Geodetic Science

Report No. 285

GLOBAL ANOMALY AND UNDULATION RECOVERY USING GEOS-3 ALTIMETER DATA

(NASA-CR-158805) GLOBAL ANOMALY AND UNDULATION RECOVERY USING GEOS-3 ALTIMETER DATA Final Report (Ohio State Univ. Research Foundation) 54 p HC A04/MF A01 CSCL 08E G3/46

N79-28824

Unclas 29363

by

Richard H. Rapp

Final Report

Prepared for

National Aeronautics and Space Administration
Goddard Space Flight Center
Greenbelt, Maryland 20770

Grant No. NSG 5275

The Ohio State University
Research Foundation
Columbus, Ohio 43212

May 1979

The Ohio State University
Research Foundation
1314 Kinnear Road
Columbus, Ohio 43212

REPORT TRANSMITTAL
MEMORANDUM

MPN: 761103

DATE: August 3, 1979

RF Project No.: 711118

Type of Report: Final

Shipped by: Certified Mail

TO: NASA Scientific and Technical Information Facility
P. O. Box 8757, Baltimore/Washington International Airport
Maryland 21240

Enclosed are one*/plus one Repro copy copies of the referenced report entitled:

Final dated May 1979 "Global Anomaly and Undulation Recovery Using Geos-3 Altimeter Data"

prepared under __ Contract X Grant No. NSG 5275

Thank you for your support of this research effort.

*cc: NASA Tech. Officer + 3 copies of report
cc: Genevieve E. Wiseman, Grants Officer

Schwerin

Chester E. Ball ge.

Chester E. Ball, Director-Reprographics,
for
The Ohio State University Research Foundation

Form RE-004 *(Rev. 5/79)*

Distribution: Sponsor, RF Administrator, Principal Investigator, File

Abstract

This report describes the analysis of 3275 Geos-3 arcs of altimeter data containing 624670 frame averages. This data was adjusted to remove orbit error and altimeter bias in a primary adjustment and four regional adjustments. The root mean square crossover discrepancy was about ±55 cm after the adjustment. The adjusted altimeter data, now considered to give geoid undulations, was used to predict values at 1° intersections from which an oceanic geoid map, with predicted accuracies, was prepared at a two meter contour interval. This geoid was compared to the GEM 9 geoid over very long profiles to examine the long wavelength error in the altimeter geoid. At a wavelength of 13010 km the root mean squares difference was 57 cm. The altimeter geoid was also compared to altimeter geoids fixed by precise orbits. We found a root mean square difference of about 1 m with a systematic difference that implied the equatorial radius of the earth was 6378137 meters.

The adjusted altimeter data was also used to determine a total of 29479 1° x 1° anomalies (and undulations), 27466 of which had an accuracy of 15 mgals or better. Their average accuracy was 8 mgals. In addition, 957 5° mean anomaly and undulation values were computed. Representative anomaly differences with terrestrial estimates were 12 mgals for the 1° x 1° values and 7 mgals for the 5° values. Additional computations of point anomaly values were made to compare with ship data in the area of the Ninety East Ridge. There we found the altimetry anomalies followed quite well variations of the anomalies at 100 km wavelengths, and clearly showed correlation with bathymetry.

Foreword

This report was prepared by Richard H. Rapp, Professor, Department of Geodetic Science, The Ohio State University. This work was supported, in part, through NASA Grant No. NSG 5275, The Ohio State University Research Foundation Project No. 711118. The grant supporting this research is administered through the Goddard Space Flight Center, Greenbelt, Maryland with Dr. David Smith as Technical Officer.

Acknowledgment

The author is very indebted to a number of persons who helped in carrying out this research. Mr. Edward Herbrechtsmeier carried out the altimeter data handling, arc merging, and the adjustment to remove orbit and altimeter bias. He also prepared a number of computer programs used in the study. Mr. Kostas Katsambalos carried out extensive programming support in arranging the predicted anomaly data and in other areas. Mr. Kamil Eren carried out a number of spectral analyses discussed in this study. Ms. Pamela Pozderac prepared the global altimeter geoid maps reproduced in the appendix from small maps made available to her. In addition Tony Watts provided ship gravity data and bathymetry for comparison with our altimetry computations.

For certain computations, computer funds were made available through the Department of Geodetic Science for use at the Instruction and Research Computer Center at The Ohio State University.

Table of Contents

Introduction

This report is an extension of the analysis with Geos-3 altimeter data described in Rapp (1977a). This extension was primarily oriented to processing an additional set of Geos-3 altimetry received during January and February 1978. As will be described in subsequent sections this new data was merged with the previous data and used to obtain a near global oceanic geoid map and a large number of $1^\circ \times 1^\circ$ mean anomalies. In addition a number of computations involving point gravity anomalies was carried out for comparisons with actual ship measurements.

The Data Set

The data used in our investigations is the intensive mode data where we use frame averages. (A frame average represents a mean over 2.048 seconds or 3.277 seconds.) In taking the original data supplied by NASA (through the Wallops Flight Center), an editing procedure is used that has six different edit criteria. These criteria are designed to remove most of the bad or poor altimetry data. In our first analysis (ibid, 1977a), we accepted 1976 arcs containing 419,294 frame measurements. The location of this edited data is shown in Figure 1.

During January and February 1978 a set of approximately 70 tapes were received containing additional Geos-3 altimeter data. The location of this unedited data is shown in Figure 2.

Portions of the data were arcs that were just the continuation of previous arc segments. A procedure was developed to merge common, continuous arcs, of the old and new data sets whenever possible. After editing and merging, the altimeter data set available for further processing is shown in Figure 3. This data set now contained 3275 Geos-3 arcs with about 624670 frame averages. The same data set is shown in Figure 4 which also shows the location and numbering of the 5° equal area anomalies used in this study.

Bias Removal and the Adjustment Process

The altimeter data that is available in the edited form is subject to errors caused by a bias in the altimeter and orbit errors. These errors must be removed (as much as possible) before additional processing is carried out. To do this a procedure was described in Rummel and Rapp (1977) and Rapp (1977a) that combined a fit of the altimeter implied geoid undulations to a satellite derived geoid with crossover constraints to obtain parameters of an error polynomial. After these parameters are found for each arc, adjusted geoid heights can be found. (We note here that formally we are dealing with sea surface heights. If we neglect sea surface topography geoid heights would be found.)

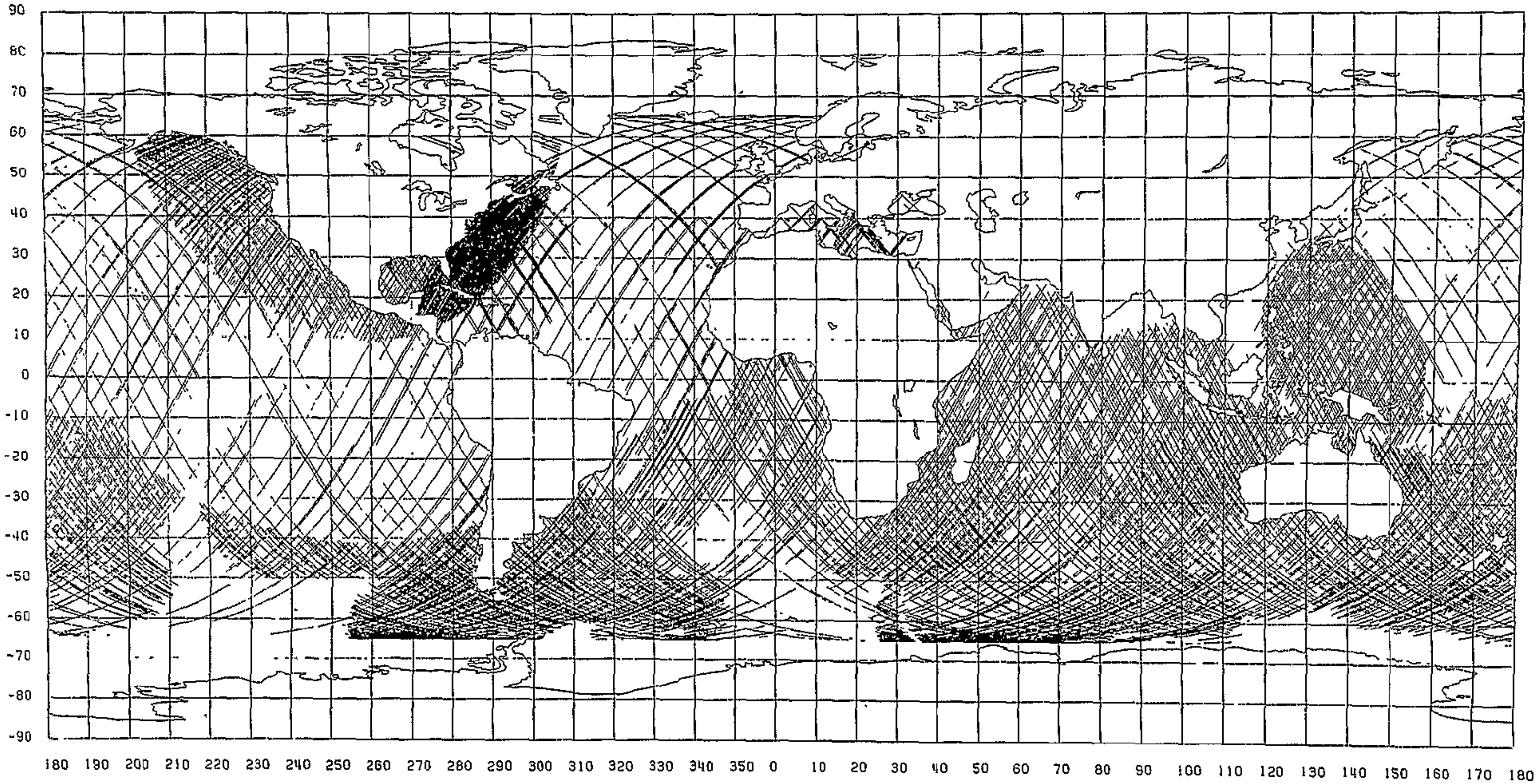

Figure 1. Location of Edited Arcs in First Altimeter Analysis (Rapp, 1977a).

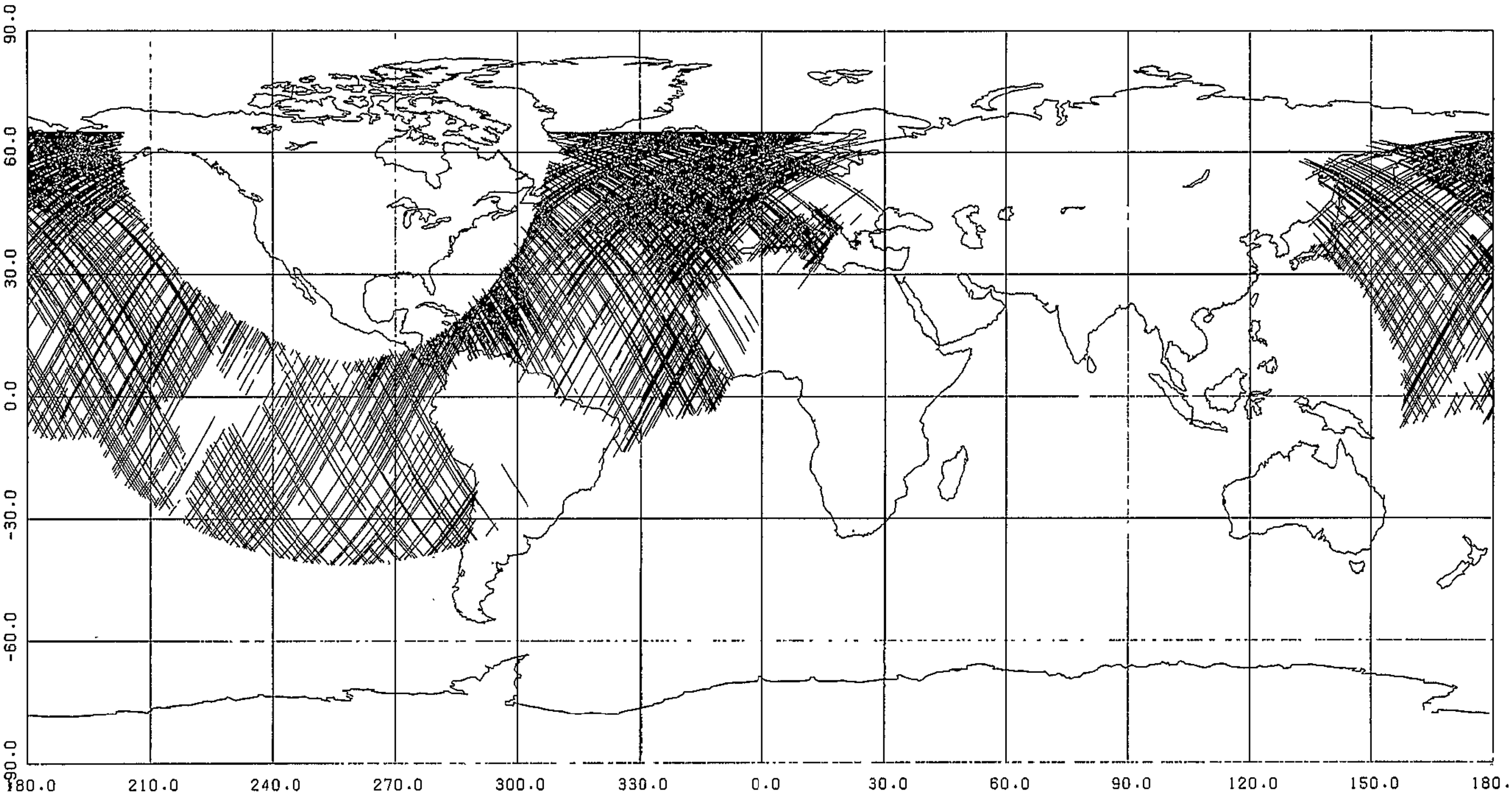

Figure 2. Location of Additional Unedited Altimeter Arcs.

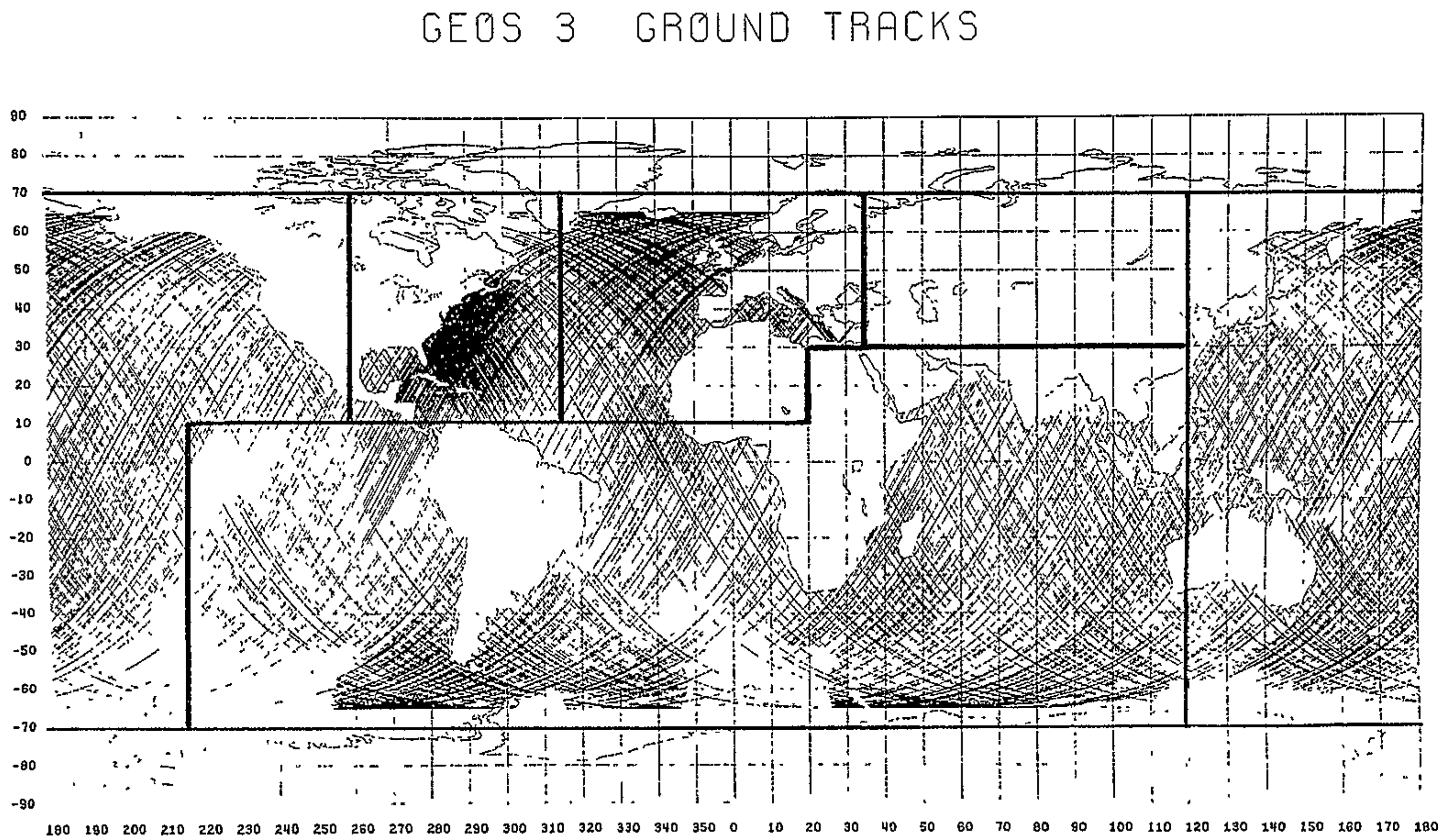

Figure 3. Location of Edited Geos-3 Altimeter Data and Areas of Regional Adjustments.

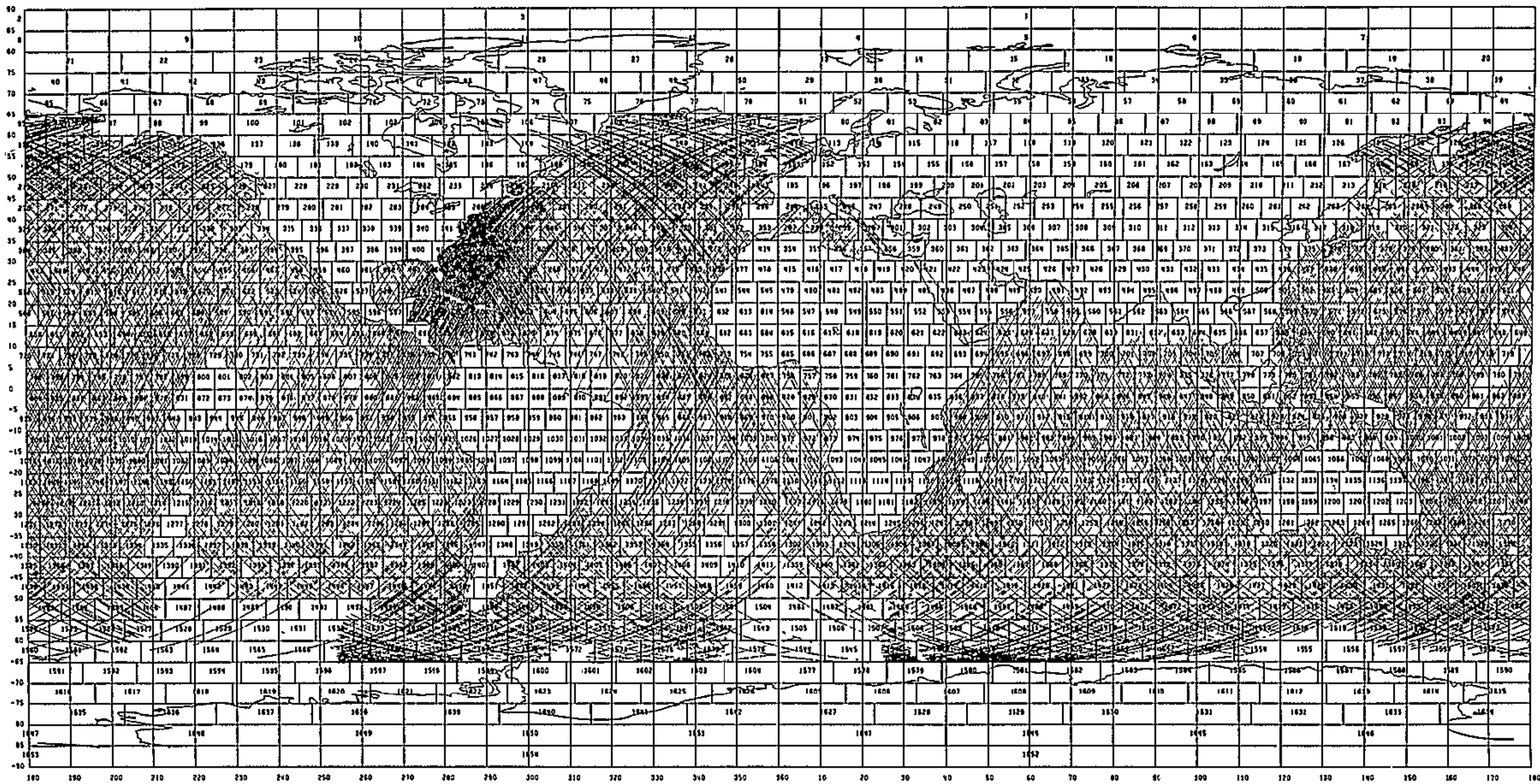

Figure 4. Location of Edited Geos-3 Arcs and 5° Equal Area Blocks.

For this work a procedure almost identical to that described in the earlier work (ibid, 1977a) was carried out. We first made an adjustment of a primary network of altimeter arcs that were chosen for their arc length and representative global distribution. After these arcs were adjusted, four regional adjustments were performed enforcing the primary arcs in the region.

The mathematics of the adjustment process are described in detail in Rapp (1977a) as well as the procedures for determining the crossover locations. The reference field used for the reference geoid was the GEM 9 (Lerch et al. 1977) set of potential coefficients taken to degree 20. For arcs whose length were less than 18° (305 seconds) only a single bias term was solved for. For the longer arcs a bias term and a trend term were found.

The location of the regional adjustments are given in Table 1 and shown in Figure 3.

Table 1. Regional Adjustment Locations

Name	Geographic Limits	
	φ°	λ°
New Calibration	70 to 10	260 to 314
East Atlantic	70 to 10	314 to 34
Africa - India	30 to 10	20 to 120
	10 to 70	218 to 120
Pacific	70 to -70	120 to 218
	70 to 10	218 to 260

Information on the adjustment of the primary and regional networks is given in Table 2.

Table 2. Adjustment Statistics Related to the Primary and Regional Adjustments.

Region	Number of				Crossover Discrepancies	
	Arcs	Unknowns	Observations	Crossovers	a priori	a posteriori
Primary	700	1383	263077	10149	± 7.81 m	± 0.60 m
New Calibration	478	800	81822	35403	6.94	0.47
East Atlantic	273	464	47065	9144	8.56	0.56
Africa - India	588	1074	139772	15977	7.42	0.50
Pacific	408	707	95947	12041	10.38	0.60

We should note here that the adjustment process is carried out in two stages. A preliminary adjustment is made and adjusted crossover discrepancies are examined. Cross points having discrepancies greater than about 3.5 meters are deleted. In some cases a whole arc segment may be deleted. The adjustment is then repeated a second time to obtain the data given in Table 2.

The crossover discrepancies after the adjustment, as shown in Table 2, are of the same magnitude as found in the first adjustment (Rapp, 1977a, Table 10).

The adjusted undulations from this new adjustment (with additional data) were compared to the corresponding values from the earlier adjustment. The results of these comparisons are given in Table 3.

Table 3. Comparison of Adjusted Point Geoid Undulation of New and Old (Rapp, 1977a) Adjustments.

Area	Number of Arcs	Mean Difference	RMS Difference	Maximum RMS Difference *
Primary	337	0.06 m	±0.33 m	±2.04 m
Calibration	154	-0.09 m	±0.29 m	±1.78 m

* Along any one arc.

We see that on the whole the differences between the adjustments is on the order of 30 cm (RMS) although over a few arcs the differences may reach the 2 meter level.

The Altimeter Geoid

Disregarding sea surface topography effects, we may regard the adjusted altimeter data to give us geoid undulations with respect to an ellipsoid of defined flattening (1/298.256) but whose equatorial radius is specifically undefined. It's conceptual definition is, however, the equatorial radius of the ellipsoid for which the global mean geoid undulation is zero.

A global oceanic geoid (or mean sea surface) has been computed from the adjusted data using primarily the procedure described by Kearsley (1977). This procedure predicts a geoid undulation (and its accuracy) at grid intersections from the surrounding point altimeter undulations. The predictions were made using least squares prediction techniques using covariances from subroutine COVA (Tscherning and Rapp, 1974) and including the data noise (with a ±0.4 m contribution from the effect of errors in the GEM 9 potential coefficients on the adjusted geoid) in the process. The grid interval chosen was $1^\circ \times 1^\circ$ using the 5 closest altimeter points. Choosing the grid interval this large can result in

the loss of detailed features below the scale of 100 km. However, the cost of computing a global oceanic geoid at a finer scale is prohibitive for us.

The grid values were contoured using a new contouring program developed by Sünkel (1979) that uses spline functions to obtain smoother contours than seen in Kearsley (1977). The computations were made, roughly, in 30°x 30° blocks. All grid undulations and their accuracies were printed out and are available for other use. The result of the contouring (for the undulations and the accuracies) were output from a small (11" wide) Versatec plotter. The individual blocks were fitted together to produce four map sheets (undulation and accuracy maps for the Eastern and Western Hemispheres) whose original size was approximately 39" x 28". Reduced versions of these maps are shown in Figures 5, 6, 7, and 8. Almost full size prints of these maps have also been made. Areas that are blank on these maps did not have sufficient altimeter data for preparing a geoid plot.

No attempt here is made to interpret this geoid. The features obvious from potential coefficient geoids is present as are the details from short wavelength geophysical structures.

Geoid Comparisons

It is of interest to compare the geoid given in Figures 5 and 6 (or more precisely the predicted grid values) with other sources. In the past comparisons with the altimeter geoid and some other reference geoid have been made over the relatively short arc segments of Geos-3 data. Our first interest here is to compare the GEM 9 undulations (to degree 20) to the altimeter derived undulations in long profiles having a constant latitude or a constant longitude. For a number of different tests 7 long (~14000 km) profiles were chosen. A plot of the GEM 9 geoid and the adjusted altimeter geoid for two typical profiles (two and five) are shown in Figures 9 and 10. (The origin for profile two is at $\lambda = 10°$, while the origin for profile five is at $\varphi = -65°$.) Information on these profiles is given in Table 4.

Table 4. Comparison of GEM 9 and Altimeter Geoid Profiles.

Profile:	Latitude	Longitude	Length	Mean Diff.	RMS Diff.
Two	-48°	10° to 186°	14732 km	-0.6 m	±2.3 m
Five	-65° to 52°	335°	14455 km	0.7 m	±2.6 m

These plots do not reveal any significant systematic differences between the two undulation sets.

The undulation differences (GEM 9 minus altimeter derived) were analyzed by Eren (1979, private communication) to determine their power spectrum. The

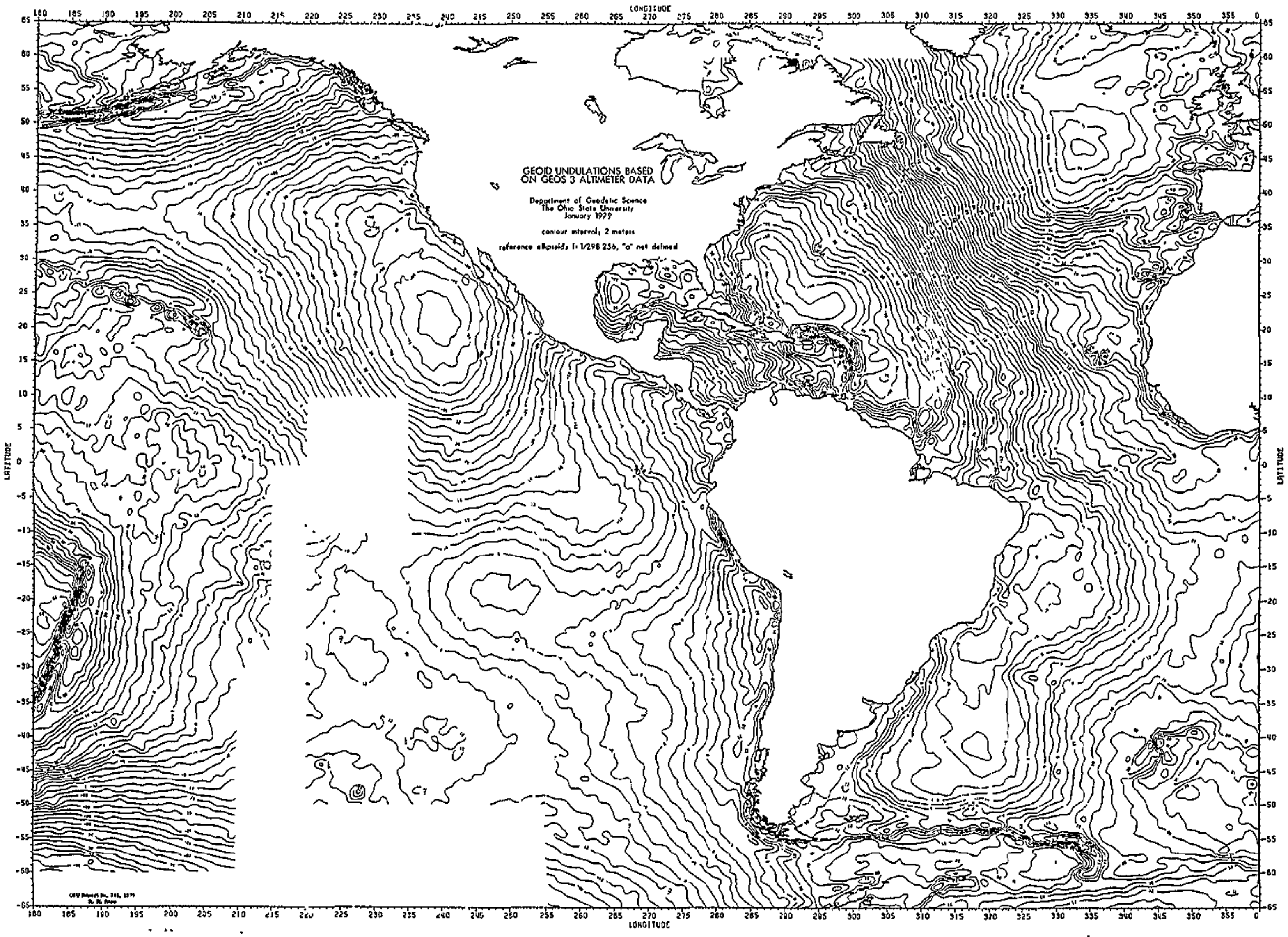
GEOID UNDULATIONS BASED ON GEOS 3 ALTIMETER DATA
Department of Geodetic Science
The Ohio State University
January 1979
contour interval; 2 meters
reference ellipsoid; f = 1/298.256, "a" not defined
LONGITUDE
LATITUDE

Figure 5.

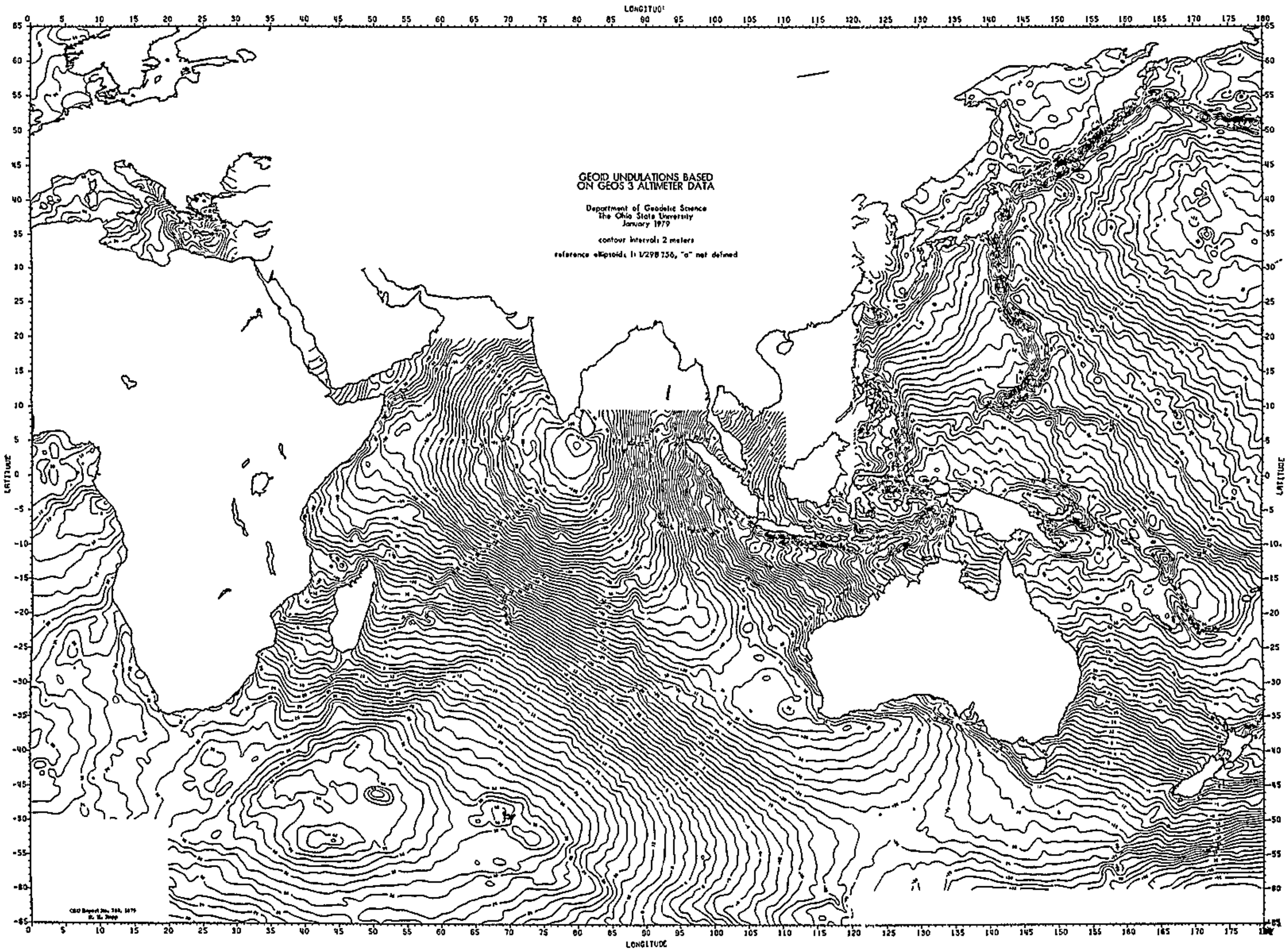
LONGITUDE
LATITUDE
GEOID UNDULATIONS BASED
ON GEOS 3 ALTIMETER DATA
Department of Geodetic Science
The Ohio State University
January 1979
contour interval: 2 meters
reference ellipsoid: f: 1/298.256, "a" not defined

Figure 6.

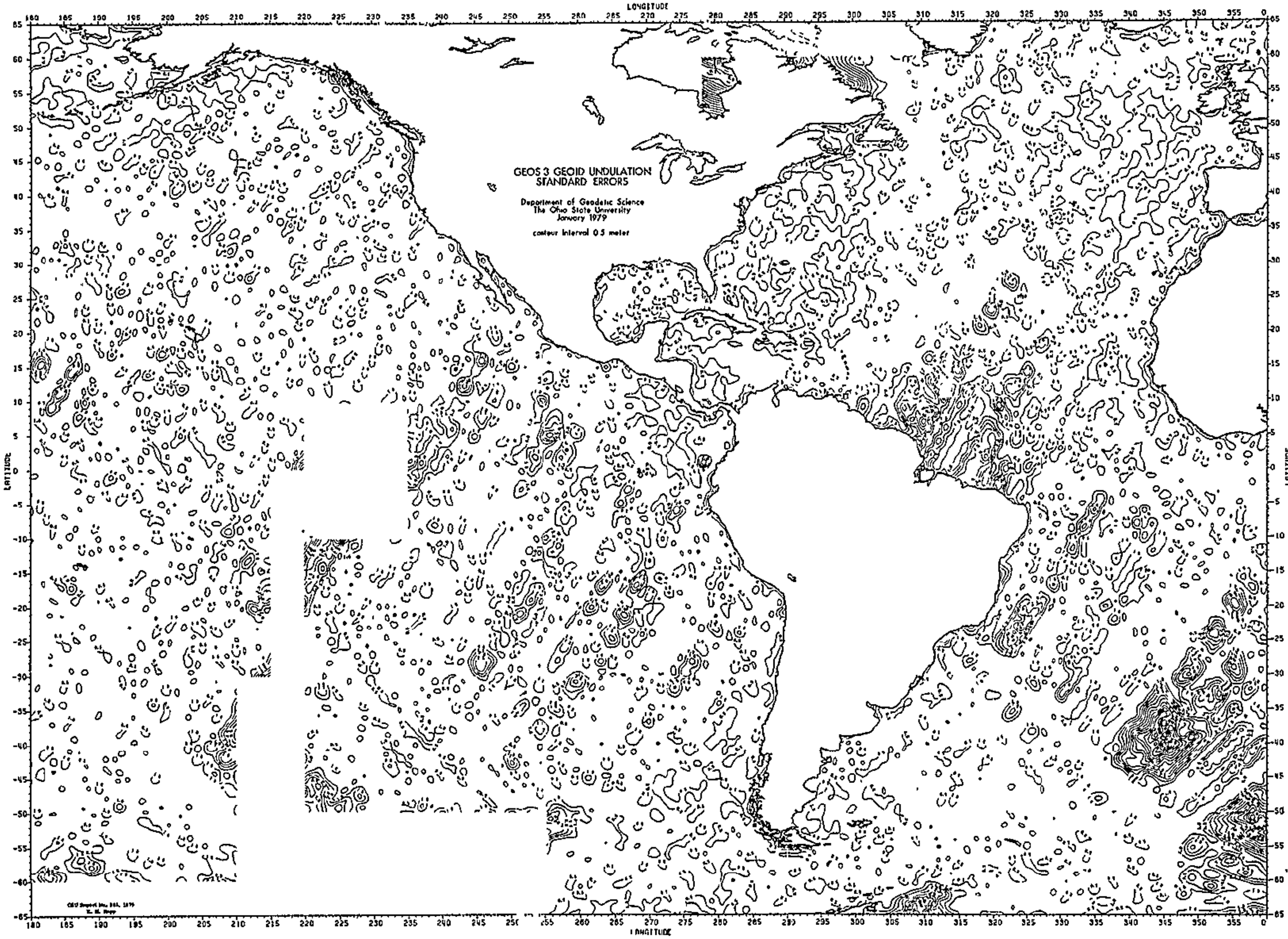
LONGITUDE
LATITUDE
GEOS 3 GEOID UNDULATION
STANDARD ERRORS
Department of Geodetic Science
The Ohio State University
January 1979
contour interval 0.5 meter

Figure 7.

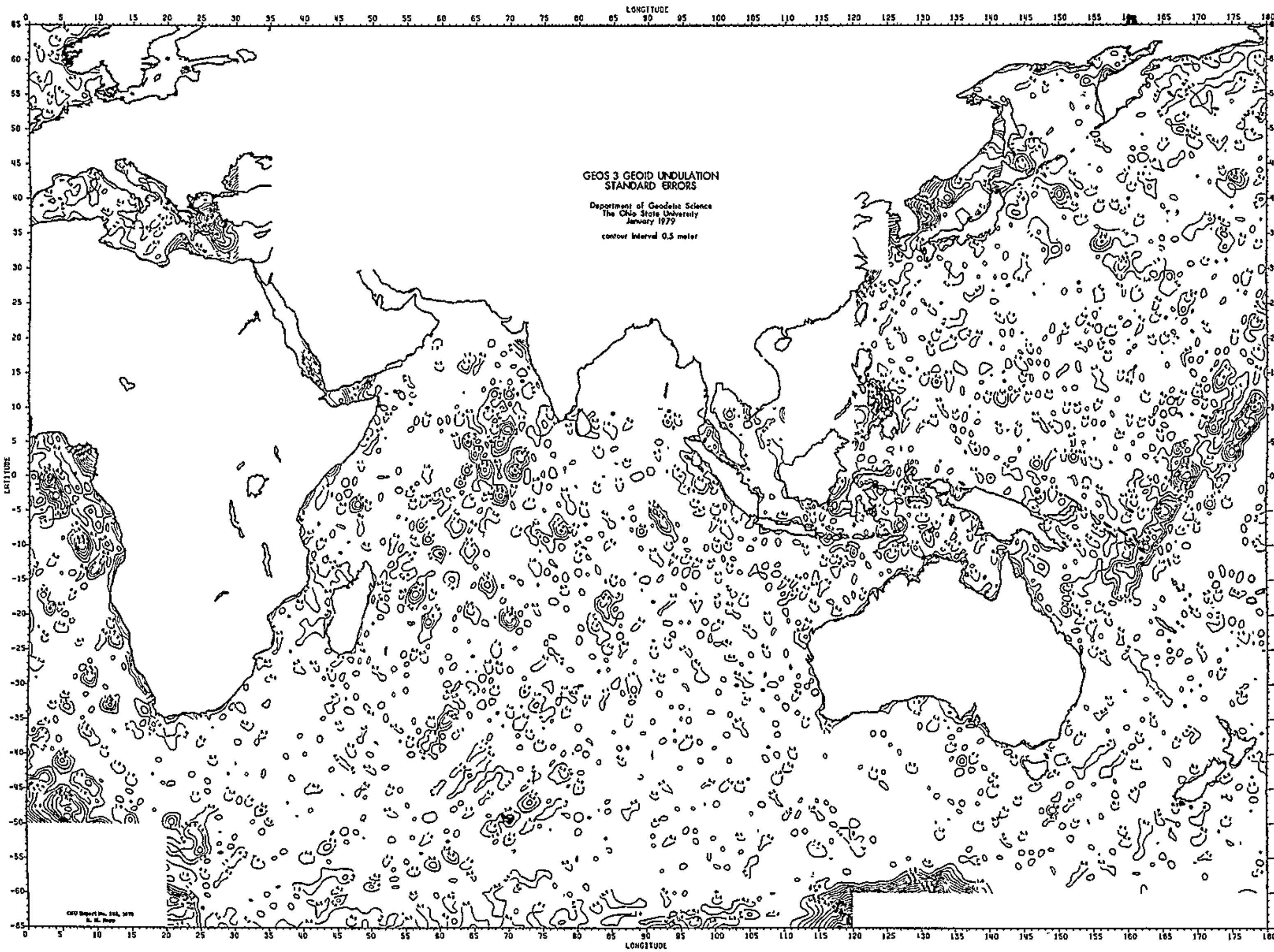
GEOS 3 GEOID UNDULATION
STANDARD ERRORS
Department of Geodetic Science
The Ohio State University
January 1979
contour interval 0.5 meter
LONGITUDE
LATITUDE

Figure 8.

Figure 9. The GEM 9 and Altimeter Undulation Along the -48° Parallel (Profile Two).

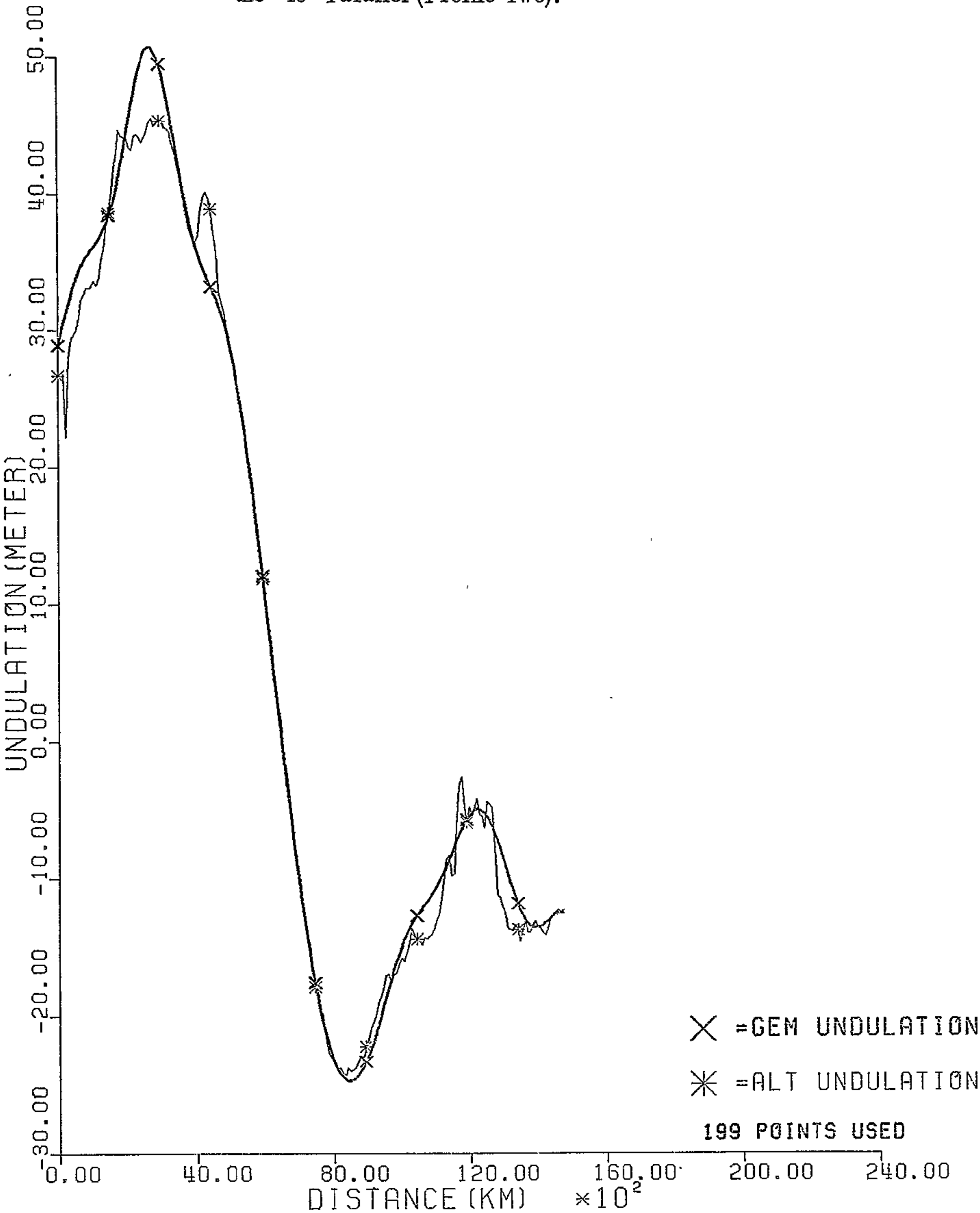

Figure 10. The GEM 9 and Altimeter Undulation Along the 335° Meridian (Profile Three).

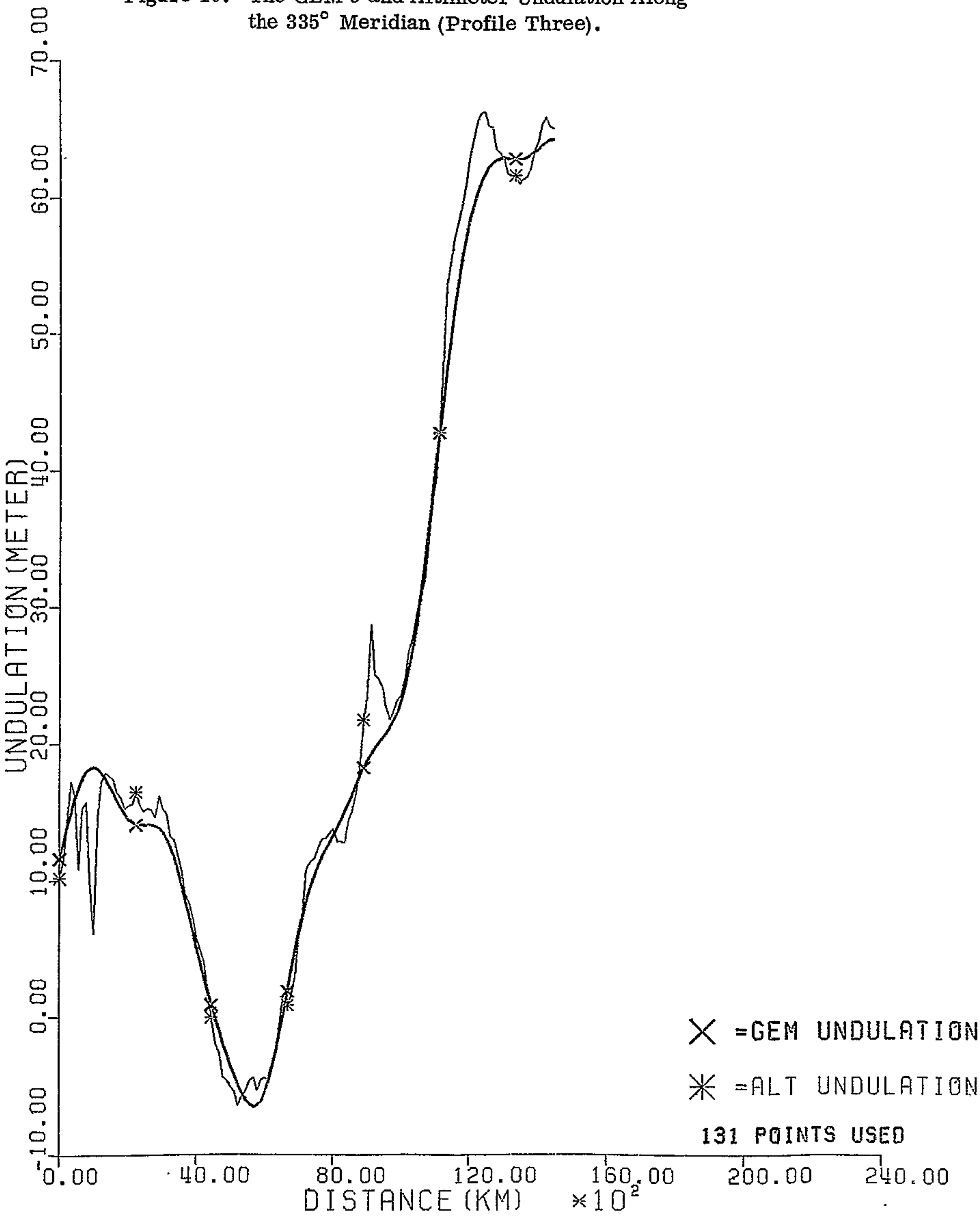

power, by wavelength is given in Table 5 based on averaging the results for the 7 individual profiles.

Table 5. GEM 9 Minus Altimeter Geoids by Wavelength.

Wavelength (km)	Approx. S.H. Degree	Power (m^2)	$(Power)^{\frac{1}{2}}$ (m)	GEM 9 Error (m)
13010	3	.33	±.57	±.04
6505	6	.61	.78	.16
4337	9	.60	.77	.38
3253	12	.58	.76	.43
2602	15	.49	.70	.51
2168	19	.15	.39	.53
Total to S.H. Degree 19		2.76	1.7	1.7 m*

* Due to errors in the GEM9 potential coefficients from n = 2 to n = 19.

The above computation assumed that the data was regarded as periodic. An alternate procedure assuming non-periodic data, with a window function was also carried out with similar results.

From Table 5 we see that at long wavelengths we can expect errors in our altimeter geoid up to about 0.75 meters. At shorter wavelengths (2168 km) the difference is similar to the expected error.

Additional computations could be carried out in this area by using more profiles and introducing data noise.

Our altimeter geoid was also compared to altimeter geoids presented by Brace (1977) and by Marsh et al (1978). The Marsh et al geoid (or mean sea surface) is based on the computation of certain laser reference orbits which are used to obtain reference altimeter undulations. These latter undulations are then used as a frame for a crossing arc adjustment process. The comparisons were made for the three areas in Marsh et al where the plotted contour interval was 1 meter. The values at grid intersections were read from the contour maps of Marsh, and taken as the predicted values from our data. The results are given in Table 6.

Table 6. Geoid Comparison from Various Sources.

Author	Area	Mean Diff. Auth. - Rapp	Standard Deviation
Marsh et al.	West. Atlantic	-3.3 m	±0.7 m
Marsh et al.	NE Pacific	-3.2	±1.1
Marsh et al.	SW of Aust.	-2.1	±1.0
Brace (1977)	5 areas	4.6	±1.1

The Brace undulations are based on Doppler satellite orbits and on a crossing arc adjustment process.

The mean differences can be due to equatorial radius used as a reference (6378140 m for Marsh, and 6378135 m for Brace) and/or an uncorrected bias term. We will assume the bias has been correctly considered in Marsh while a correction of 2.5 m is to be subtracted from the Brace data (Anderle, 1979). The resultant mean differences then will imply an ideal equatorial radius as given in Table 7.

Table 7. Equatorial Radius Implied by the Altimeter Geoid Comparisons.

Comparison with:	Equatorial Radius
Marsh et al	6378137.1 m
Brace	6378137.1 m

The agreement of the two values is fortuitous. We must remember, however, that these values assume the orbit scale is correct. A formal accuracy assessment was not carried out but ±2 meters seems reasonable.

The Computation of Mean Covariance Functions

The estimation of the mean anomalies and mean undulations was to be done by the method of least squares collocation using the procedures described in Rapp (1977a). As part of these procedures it is necessary to determine point and mean covariance functions. As originally used in Rapp (ibid) the mean covariance functions were determined from the numerical integration of point covariance functions. An alternative method, used earlier (Tscherning and Rapp, 1974), by Schwarz (1976) and others, is to introduce the smoothing operator for degree ℓ, β_ℓ (Meissl, 1971) into the series expressions for the needed covariance functions. The mean covariances needed were $\text{cov}(\overline{\Delta g},\overline{\Delta g})$, $\text{cov}(N,\overline{\Delta g})$, and $\text{cov}(N,\overline{N})$ where an unbarred quantity represents a point value and a barred quantity represents a mean value. In our test computations we shall restrict the mean value to a $1^\circ \times 1^\circ$ anomaly block

A point anomaly covariance function, given with respect to a reference field of potential coefficients to degree ℓ (ref) can be computed from (Tscherning and Rapp, 1974):

$$\text{cov}(\Delta g,\Delta g) = \sum_{\ell=\ell(\text{ref})+1}^{\infty} c_\ell \, s^{\ell+2} \, P_\ell(\cos\psi) \tag{1}$$

where c_ℓ are anomaly degree variances and $s = (R_B/R)^2$ where R_B is the radius of the Bjerhammer sphere (internal to the earth) and R is the mean radius of the earth. One estimate for s is 0.999617 (Tscherning and Rapp, 1974). To obtain the mean covariances we introduce β_ℓ:

$$\operatorname{cov}(\bar{\Delta}g,\bar{\Delta}g) = \sum_{\ell=\ell(\mathrm{ref})+1}^{\infty} c_\ell\, \beta_\ell^2\, s^{\ell+2}\, P_\ell(\cos\psi) \tag{2}$$

The smoothing operator β_ℓ can be computed from the following (Rapp, 1977b)

$$\beta_\ell = \cot\frac{\psi_0}{2}\;\frac{P_{\ell 1}(\cos\psi_0)}{\ell(\ell+1)} \tag{3}$$

where ψ_0 is the radius of a cap that has the same area as the block (e.g. $1^\circ\mathrm{x}\,1^\circ$) being considered. As we are dealing with $1^\circ\mathrm{x}\,1^\circ$ values the areas will be latitude dependent so that β_ℓ, in our application, will be latitude dependent.

The other covariances needed can be found by the law of propagation of covariances (Moritz, 1972, 1978). In spherical approximation we have:

$$\operatorname{cov}(N,\bar{\Delta}g) = (R/G) \sum_{\ell=\ell(\mathrm{ref})+1}^{\infty} c_\ell/(\ell-1)\, \beta_\ell\, s^{\ell+1}\, P_\ell(\cos\psi) \tag{4}$$

$$\operatorname{cov}(N,\bar{N}) = (R/G)^2 \sum_{\ell=\ell(\mathrm{ref})+1}^{\infty} c_\ell/(\ell-1)^2 \beta_\ell s^{\ell+1}\, P_\ell(\cos\psi) \tag{5}$$

where G is an average value of gravity. In actual computations the summation to ∞ was replaced by a summation to degree 540 which is sufficiently high so that no significant change will take place by going to a higher degree. Tables of these mean covariances were constructed at 0.°05 intervals. The original program was modified by removing the numerical integration procedure for the $1^\circ\mathrm{x}\,1^\circ$ block computations and replacing it with table interpolation procedures.

These methods were tested by carrying out predictions in two 5° equal area anomaly blocks both of which had a north latitude of -10°. The series covariance functions were computed with a β value for $1^\circ\mathrm{x}\,1^\circ$ blocks at the equator. Predictions were carried out using the numerical integration procedure and the directly tabulated mean covariance functions. The differences in the $1^\circ\mathrm{x}\,1^\circ$ mean anomaly predictions was about ±0.6 mgals while the mean undulation differences were on the order of ±.1 m. The estimated standard deviations were essentially unchanged. We thus conclude that this procedure could be applied successfully.

The computer time savings were clearly seen in a run where the error covariance matrix (see later discussion) was also computed. The savings was 14 secs (on an IBM 370/168) or approximately 8% of the total time. This is a representative value only as the specific savings will depend on the number of given data points (alternate undulations).

Although the savings could be significant over repeated computations, the decision was made not to implement these procedures in our operational runs. One reason for this is that we felt that we would have to compute new covariances for different latitude areas because of the change in β's with the area of the block. (For example, for a $1^\circ\mathrm{x}\,1^\circ$ at the equator β = 0.°564 while at latitude

$60°$, $\beta = 0°.402$.) It could be that sufficient accuracy could be found by adopting some average β values but this was not tried. Additional testing in this area is needed as well as the testing of series expression for the 5° equal area predictions that were also carried out.

The Error Covariance Matrix

In the computations performed previously (Rapp, 1977a) for mean anomalies and undulations, the 1°x 1° values within a 5° equal area block were predicted from the same data set selected in and around the 5° block. This procedure had the advantage that only one matrix inversion was required; it did however have the disadvantage that the predictions of the 1°x 1° blocks could be highly correlated. To specifically consider this question we considered the following expression for the error-covariance matrix for the least squares collocation procedure (Moritz, 1972):

$$E_{ss} = C_{ss} - C_{sx} \bar{C}^{-1} C_{xs} \qquad (6)$$

where: E_{ss} is the error covariance matrix of the signals being predicted;
C_{ss} is the (physical) covariance matrix of the signals being predicted;
C_{sx} is the cross covariance matrix between the signals being predicted and the observations;
$\bar{C}$ is the covariance matrix of the observations plus the noise covariance matrix;
C_{xs} is C_{sx}^{T}.

In our case the observations are the altimeter derived undulations while the signals being predicted are the 1°x 1° mean gravity anomalies (or undulations). The size of the E_{ss} matrix will depend on the number of 1°x 1° blocks within the 5° equal area block. Near the equator E_{ss} would be a 25 x 25 matrix while at latitude 65° E_{ss} would be a 55 x 55 matrix. The diagonal elements of E_{ss} would be the square of the predicted accuracy of the individual blocks. E_{ss} can also be converted into a correlation coefficient matrix.

Equation (6) was evaluated for several cases of possible interest. In the first case only one known undulation value was used to estimate all the 1°x 1° anomalies in a 5° block. The maximum correlation found was 0.53. When 88 data points were used in this same 5° block, the maximum correlation coefficient was now .13.

Two additional 5° blocks were also investigated. One 5° block (at $\varphi_m = -12°.5$) had 391 data points used for the prediction. This would be considered a block with fairly dense altimeter data. In this case the largest correlation coefficient was 0.20. A second block, in the same latitude, having a less dense data set (261 points), was also considered. In this case the largest correlation coefficient reached 0.34.

We thus see that with increasing data sets the correlation between the blocks decreases. For most computations we will be doing, we would expect the correlation coefficient to be 0.3 or less. Because of this small magnitude we can regard most anomalies as almost independently determined. We therefore choose not to compute the E_{ss} matrix for our operational work.

Reference Model Error

The prediction of mean gravity anomalies and geoid undulations has been carried out with respect to a reference gravitational field model defined by the GEM 9 potential coefficients (Letch et al., 1977) taken to degree 20. Specifically the anomaly and its estimated accuracy is computed from the following equations (Rapp, 1977a, 1978a):

$$\Delta g = \underline{C}_{ghR} \left(\underline{C}_{hhR} + \underline{D} \right)^{-1} \left(\underline{h} - \underline{h}_R \right) + \Delta g_R \tag{7}$$

$$m_g^2 = \underline{C}_{ggR} - \underline{C}_{ghR} \left(\underline{C}_{hhR} + \underline{D} \right)^{-1} \underline{C}_{hgR} \tag{8}$$

where

- Δg is the predicted free-air gravity anomaly with respect to ellipsoidal gravity field;
- h is a column vector of the altimeter implied geoid undulations;
- C_{ghR} is the row vector containing the covariance (referred to the reference field) between the anomaly being predicted and the given geoid undulation;
- C_{hhR} is the square, symmetric matrix containing the covariances (referred to the reference field) between the given geoid undulations. If there are n $\underline{h}$ values being used this matrix is n x n;
- D is the error-covariance matrix of the given geoid undulations which was taken to be a diagonal matrix whose elements corresponded to the square of the standard deviation of the altimeter measurement;
- C_{ggR} the expected mean square value (referred to the reference field) in a global sample, of the anomaly being predicted;
- m_g the predicted standard deviation of the predicted anomaly;
- Δg_R, N_R, h_R the gravity anomaly and geoid undulation implied by the reference set of potential coefficients.

Similar equations can be written for the estimation of the mean undulations.

In our previous computations no consideration was given to the error in the final result caused by errors in the GEM 9 coefficients. One way suggested by Colombo (private communication, 1979) is to add to the covariance matrices, given with respect to the reference field, a component implied by the errors in the potential coefficients. This component can be obtained from equation (2), (4), and (5) by setting $\beta_\ell = 1$ and replacing the c_ℓ values by the errors in the anomaly degree variances implied by the errors in the potential coefficients.

Such a computation was done and prediction results for the $1^\circ \times 1^\circ$ anomalies and undulations in a 5° block were compared. We found changes in the predicted $1^\circ \times 1^\circ$ anomalies of only about ± 0.2 mgals with the standard deviations increasing about 0.3 mgal (from about ± 7 mgal). The undulation values and their accuracy changed no greater than 0.2 meter.

We thus conclude this the errors in the GEM 9 coefficients, when used as a reference field, do not significantly contribute, to our final error estimate, provided the above procedure is correct.

Anomaly Differences Implied by the New and Old Adjustments

In our previous report we had computed 9995 $1^\circ \times 1^\circ$ anomalies. By February 1978 this number had increased to 12144 values, all values being based on the adjusted undulations from our first adjustment process. After completing the second adjustment of the altimeter data we computed a large number of $1^\circ \times 1^\circ$ anomalies to compare with our earlier estimates. Some statistics on these comparisons are shown in Table 8.

Table 8. Comparison of $1^\circ \times 1^\circ$ Mean Anomalies Computed from New and Old Adjustments of the Altimeter Data.

Area *	Number	Mean Diff.	RMS Diff. (mgals)	Max. Diff. (mgals)
Calibration	489	0.2	±4.9	34.3
South America	1675	0.2	±2.3	17.2

* see Rapp (1977a)

The root mean square differences are all smaller than the predicted accuracy of the $1^\circ \times 1^\circ$ anomalies and thus such differences are not of great concern. There is some concern over a few large discrepancies (such as the 34 mgal difference). The reason for this is not clear although it may be related to a singly bad data point.

The anomalies from the new and old adjustment were also compared to terrestrial anomalies. These comparisons are shown in Table 9.

Table 9. Comparison of $1^\circ \times 1^\circ$ Mean Anomalies from the New and Old Adjustment to Terrestrial Data.

Area	Old Adjustment		New Adjustment	
	Number	RMS Diff.	Number	RMS Diff.
Calibration	260	± 8.9 mgals	265	± 10.7 mgals
South America	382	16.5	491	17.7
Alaska	492	9.5	524	10.5
Phillippines	527	12.5	194	12.4

It seems clear that the old adjustment yields slightly better anomaly values. Again considering the predicted anomaly accuracies these differences are not significant. However they are sufficient to have us accept in our final results, anomalies predicted from the old adjustment where such data exists in sufficient quantity to obtain reliable predictions.

Effect of the Mass of the Atmosphere

The computations for the gravity anomalies made through equation (7) have made no assumption on the attraction of the mass of the atmosphere. For points internal to a spherical shell comprising the atmosphere the attraction of the atmosphere is zero. However in gravity anomaly computations the current procedure is to include the mass of the atmosphere within the mass of the reference ellipsoid. Thus for comparisons of altimeter derived anomalies with terrestrial anomalies derived using a gravity formula based on a reference ellipsoid that contains the mass of the atmosphere, a small correction to the altimeter anomaly is needed. This correction can be found by first defining a gravity anomaly with respect to an ellipsoid for which the mass of the atmosphere is not included:

$$\Delta g_E = g - \gamma_E \tag{9}$$

where E indicates the earth mass, g is observed gravity (properly reduced) and γ_E is normal gravity. The corresponding anomaly when the mass of the atmosphere is included in the reference ellipsoid is:

$$\Delta g_{E+A} = g - \gamma_{E+A} \tag{10}$$

Thus:

$$\Delta g_{E+A} = \Delta g_E - (\gamma_{E+A} - \gamma_E) \tag{11}$$

For points (or blocks) located at a zero elevation $(\gamma_{E+A} - \gamma_E)$ is 0.87 mgals. (IAG, 1971). Thus, before comparing the altimeter derived anomalies to terrestrial anomalies that would be referred to the gravity formula of the Geodetic Reference System 1967, (for example) 0.87 mgals should be subtracted from the altimeter derived anomaly.

Effect of Systematic Undulation Error on the Anomaly Predictions

The "geoid undulations" used in our estimation process may have systematic errors caused by the neglect of sea surface topography with respect to the geoid. To see the effect we carried out a computation of the $1^\circ \times 1^\circ$ anomalies and undulation in a 5° equal area block using altimeter derived undulations from which a constant 1 meter had been removed. Comparison with the same predictions without the systematic change revealed a systematic difference in the anomaly predictions of 2.5 mgals. This change is below the average accuracy of the predicted anomalies by a factor of 3.

Subsequent comparisons of the $1^\circ \times 1^\circ$ predicted anomalies to terrestrial anomalies indicates a mean difference of 0.5 mgals. This difference could be due to sea surface topography effects that do not average to zero, to an error in the equatorial gravity of the Geodetic Reference System 1967, or it may be statistically insignificant.

Effect of Covariance Functions Used on the Predicted Anomalies and Undulations

The predictions defined by equation (7) require certain covariance functions. In Rapp (1977a) the covariance functions were obtained from subroutine COVA (Tscherning and Rapp, 1974) with respect to a degree 20 field based on a certain anomaly degree variance model. The covariances used are called global covariances in the sense that they are based on parameters representative of the global gravity field. One argument is that it would be more reasonable to use covariance functions specifically designed for a given area. It thus seems appropriate to consider the sensitivity of our predictions to the covariances used in the prediction process.

To do this we choose to work with three different covariance functions carrying out predictions in $1^\circ \times 1^\circ$ blocks within several 5° equal area blocks. The first covariance function group was that implied by the anomaly degree variance model described in Tscherning and Rapp (1974). This model was used to compute the needed covariances with respect to a degree 20 reference field. These covariances were the ones used in all of our previous computations (Rapp, 1977a).

The second covariance function was based on an anomaly degree variance model developed by Jekeli (1978) and designated as the 1 L model. This model used the same form of the anomaly degree variance model as used by Tscherning and Rapp but computed the model parameters enforcing a low horizontal anomaly variance (C_0) considerably less than the T/R model, and an anomaly correlation length ξ (i.e. $C(\xi) = C_0/2$) that was about twice that of the T/R model.

The third covariance function group considered was that described by Jordan (1972) for local use. Jordan discussed a third-order Markov undulation covariance

model, from which an anomaly covariance model, and an anomaly-undulation cross covariance model could be derived. Specifically we have:

$$C(N,N) = C_0(N)\left(1 + \frac{r}{D} + \frac{r^2}{3D^2}\right) e^{-r/D} \tag{12}$$

$$C(\Delta g,\Delta g) = C_0(\Delta g)\left(1 + \frac{r}{D} - \frac{r^2}{2D^2}\right) e^{-r/D} \tag{13}$$

$$C(\Delta g, N) = \frac{2\sqrt{C_0(N)\,C_0(\Delta g)}}{\sqrt{6}}\left[\frac{r}{2D}\left(1-\frac{r^2}{2D^2}\right)\left[I_0\left(\frac{r}{2D}\right)K_1\left(\frac{r}{D}\right)\right.\right.$$
$$\left.\left. - I_1\left(\frac{r}{2D}\right)K_0\left(\frac{r}{2D}\right)\right] + \frac{r^2}{4D^2}\left[I_0\left(\frac{r}{2D}\right)K_0\left(\frac{r}{2D}\right) + I_1\left(\frac{r}{2D}\right)K_1\left(\frac{r}{2D}\right)\right]\right] \tag{14}$$

In these expressions $C_0(N)$ is the variance of the undulations and $C_0(\Delta g)$ is the variance of the anomalies in the area under consideration with respect to a reference field which is the GEM 9 field in our case. I_n is the Bessel function of the first kind of order n, and K_n is the Bessel function of the second kind of order n. (Although these functions are not defined at $r = 0$, definition is possible at a value of r sufficiently small to approximate zero.) The value of r is the distance between the points under consideration and D is known as the characteristic distance. The values of $C_0(N)$ and $C_0(\Delta g)$ are related as follows:

$$\frac{\sqrt{C_0(N)}}{\sqrt{3}\,D} = \frac{\sqrt{C_0(\Delta g)}}{\sqrt{2}\,g_0} \tag{15}$$

where g_0 is an average value of gravity (979.8 gals).

We need to develop a procedure to determine the two independent parameters of this model. To do this we use the fact that the mean anomaly (or mean undulation) variance can be computed knowing the point covariance function (Heiskanen and Moritz, 1967, p. 276). Thus, if we subdivide a given area into n^2 subdivisions we can write

$$\operatorname{var}(\overline{\Delta g}) = \frac{1}{n^4}\sum_{i}^{n}\sum_{j}^{n}\sum_{i'}^{n}\sum_{j'}^{n} C\left((\Delta g,\Delta g)\; x_i, y_j, x_{i'}, y_{j'}\right) \tag{16}$$

where x, y are coordinates within the block. A similar equation can be written for $\operatorname{var}(\overline{N})$.

Now suppose we take an area for which we known $\operatorname{var}(\overline{\Delta g})$ and $\operatorname{var}(\overline{N})$ with respect to some reference field. Then we can use these values to determine $C_0(N)$ and $C_0(\Delta g)$ by solving (16) numerically. Given these two values the characteristic distance D can be found from (15). The process is an iterative one since some starting D value is needed. In our tests, convergence was obtained in an average of 5 iterations by stopping when the change in D was less than 1 meter.

In our application we chose to find the local parameters $C_0(\Delta g)$, and D that would be characteristic of the $1^\circ \times 1^\circ$ anomalies and undulations in specific 5° equal area blocks. The data used for the computation of $\operatorname{var}(\overline{\Delta g})$ and $\operatorname{var}(\overline{N})$

was the anomaly and undulations predictions with respect to the GEM 9 field when the predictions were done with the covariances from COVA using the T/R anomaly degree variance model. Given these two values we then computed $C_0(\Delta g)$, D and $C_0(N)$ which were then used to generate the covariances from equations (12), (13), and (14).

We selected four 5° equal area blocks to work with. These blocks are numbered (see Figure 4) as follows: 1058 (a block stradling the 90° East Ridge), 1060 (a block in the Indian Ocean with mild anomaly variation with medium altimeter coverage), 602 (a block that contains the Puerto Rican Trench and has dense altimeter coverage), and block 465 (off the east coast of the United States with dense altimeter coverage).

The values of $\sqrt{C_0(N)} = \sigma_N$, $\sqrt{C_0(\Delta g)} = \sigma_g$, D, and the anomaly correlation distance (i.e. the distance at which $C(r) = C_0(\Delta g)/e^{-1}$ $(1/e = .3678\ldots)$). These values (except for D) are also given, for comparison purposes, for the COVA covariances with the T/R anomaly degree variance model, and the 1L model of Jekeli.

Table 10. Parameters of Covariance Functions.

Block/ Function	σ_g mgals	σ_N meters	D meters	Anomaly Correl. Dist. (km)
1058	16.09	1.28	64042	88
1060	11.34	3.00	212365	289
602	121.88	7.11	46841	64
465	26.55	2.10	63637	87
COVA	38.98	3.64	-	199
1L	31.97	3.62	-	154

The large σ_g value for block 602 reflects the very large (about -250 mgal) anomalies associated with the Puerto Rican Trench.

For blocks 1058, 1060, and 602 predictions were carried out with the three different covariance functions. For block 465 only the COVA with T/R model and the Jordan model were used.

The predicted anomalies were then compared to corresponding terrestrial estimates to see if one covariance function gave better predictions than another. The root mean square (RMS) differences, the RMS terrestrial anomaly standard deviation, and the RMS altimeter derived anomaly standard deviation are given in Table 11.

Table 11. Comparison of $1^\circ \times 1^\circ$ Anomalies Derived Using Different Covariance Functions to Terrestrial Estimates.

Block Number 1058; RMS Terrestrial Anomaly S.D. = ±10.8 mgals		
Covariance	RMS Difference (mgals)	RMS Alt. Anomaly S.D. (mgals)
COVA	±12.7	±7.6
Jekeli 1 L	12.7	6.5
Jordan	12.0	4.8

Block Number 1060; RMS Terrestrial Anomaly S.D. = ±10.6 mgals		
Covariance	RMS Difference (mgals)	RMS Alt. Anomaly S.D. (mgals)
COVA	±11.9	±6.8
Jekeli 1 L	11.9	5.6
Jordan	11.9	2.4

Block Number 602; RMS Terrestrial Anomaly S.D. = ±11.8 mgals		
Covariance	RMS Difference (mgals)	RMS Alt. Anomaly S.D. (mgals)
COVA	±12.2	±6.3
Jekeli 1 L	12.4	5.1
Jordan	12.1	9.7

Block Number 465; RMS Terrestrial Anomaly S.D. = ±13.8 mgals		
Covariance	RMS Difference (mgals)	RMS Alt. Anomaly S.D. (mgals)
COVA	±9.0	±6.4
Jordan	9.6	4.7

From Table 11 we see that no significant improvement or difference in the prediction results can be seen from the use of different covariance functions. The most significant change occurs in the predicted accuracy of the anomalies where the Jordan function displays accuracies more related to the variations of the anomaly field in a specific area.

We have also compared the anomalies from the Jekeli 1 L function and the Jordan function to the anomalies from the COVA 1 L function. These comparisons are shown in Table 12.

Table 12. Comparison of the 1°x 1° Anomalies Derived from Two Alternate Covariance Functions to the Values Obtained from the Covariances of COVA.

Block	Covariance Used	Mean Diff. (mgals)	RMS Diff. (mgals)
1058	Jekeli 1L	0.0	0.3
1058	Jordan	0.1	2.3
1060	Jekeli 1L	0.0	0.1
1060	Jordan	0.7	3.0
602	Jekeli 1L	0.1	0.4
602	Jordan	-2.6	7.9
465	Jordan	-0.3	1.5

We see that the comparison with the Jekeli 1L function shows differences on the order of 0.3 mgals while the differences with the Jordan function are higher, being about ±3 mgals in three blocks rising to 8 mgals in block 602. The large differences in this latter block occur for anomalies on the order of -280 mgals, the largest difference being 20 mgals. Five specific 1°x 1° anomalies and undulations for blocks along the trench are shown in Table 13 as computed using the three different covariance functions previously discussed.

Table 13. 1°x 1° Anomalies and Undulations in the Area of the Puerto Rican Trench.

Northwest Corner						Undulations (meters)		
$\varphi°$	$\lambda°$	Terr.	COVA	1L	Jordan	COVA	1L	Jordan
20	292	-244±24	-231±6	-231±5	-243±11	-62.4±.2	-62.3±.2	-62.7±.4
20	293	-282±14	-264±6	-263±6	-284±10	-65.6±.2	-65.6±.2	-66.1±.4
20	294	-205±22	-223±7	-222±6	-239±12	-63.5±.2	-63.5±.2	-64.0±.4
20	295	-166±10	-160±6	-159±5	-172±10	-59.7±.2	-59.7±.2	-60.0±.4
20	296	-162± 6	-148±7	-149±6	-161±13	-59.1±.3	-59.1±.2	-59.5±.5

In this section we have examined the variability of the prediction process as a function of the covariances used. There are some indications that the use of a tailored covariance function may give slightly better predictions than global functions but the evidence is marginal. On the other hand the standard deviations from the use of the Jordan function may be more realistic. In some cases these standard deviations are more and in some less than obtained from the global functions. In order to apply the local function we must have representative values for the anomaly and undulation variances. In our application this was simple as predictions had already been carried out. If such predictions had not been done we could have used

the terrestrial data to obtain an anomaly variance and the results of some detailed geoid computations to obtain the undulation variance. If we were working in gravimetrically unsurveyed areas (such as the southern oceans) we could select a global function.

For our production estimation process we choose to work with the covariances implied by COVA with the T/R anomaly degree variance model. This was primarily done for consisting purposes as there did not seem to be sufficient evidence to suggest that significant gains would be obtained from using a tailored covariance function. Perhaps, with more accurate determination of oceanic mean anomalies from terrestrial data, a more definitive comparison and conclusions could be made.

Production Estimation of Mean Anomalies and Undulations

The estimation of $1^\circ \times 1^\circ$ and 5° mean anomalies (and undulation) using equation (7) took place using the old adjustment where data was sufficiently dense, and using the new adjustment data in other areas. Many of the old adjustment anomalies were taken from Rapp (1977a). The covariance function used was obtained from COVA (Tscherning and Rapp, 1974) with respect to a degree 20 field. Other specific details of the prediction process are described in Rapp (1977a). The values from the old and the new adjustment were merged together to form a combined data set. This data set contained 29479 $1^\circ \times 1^\circ$ blocks and 957 5° equal area blocks. A number of the $1^\circ \times 1^\circ$ predictions were made in land areas and in ocean areas where the altimeter data was sparse. This was done only because of the manner chosen for the estimation of <u>all</u> the $1^\circ \times 1^\circ$ anomalies within a 5° equal area block. The more reliable anomalies are those having an accuracy of ± 15 mgals or better. There are 27466 such values whose location is shown in Figure 11. (As a matter of interest Figure 12 shows the 20599 values where the accuracy is ± 8 mgals or better.) A listing of the 5° equal area anomalies and undulations, referred to an ellipsoid whose flattening is 1/298.256, is given in the appendix. A tape containing the $1^\circ \times 1^\circ$ altimeter derived anomalies is also available. The predicted anomalies have been compared to a terrestrial data set called "June 78 delete 424". This data set is that terrestrial field described in Rapp (1978b) less 424 anomalies that had a very large difference with the altimeter values. The net data set available for comparison purposes contained 38981 values. This data set was also used to generate a 5° equal area anomaly field that was used for the 5° block comparisons. The 5° comparisons were made using only those 5° terrestrial anomalies where the terrestrial standard deviation was 10 mgals or less. The $1^\circ \times 1^\circ$ comparisons were made only when the accuracy estimates for both anomalies were 15 mgals or better. The results are given in Table 14.

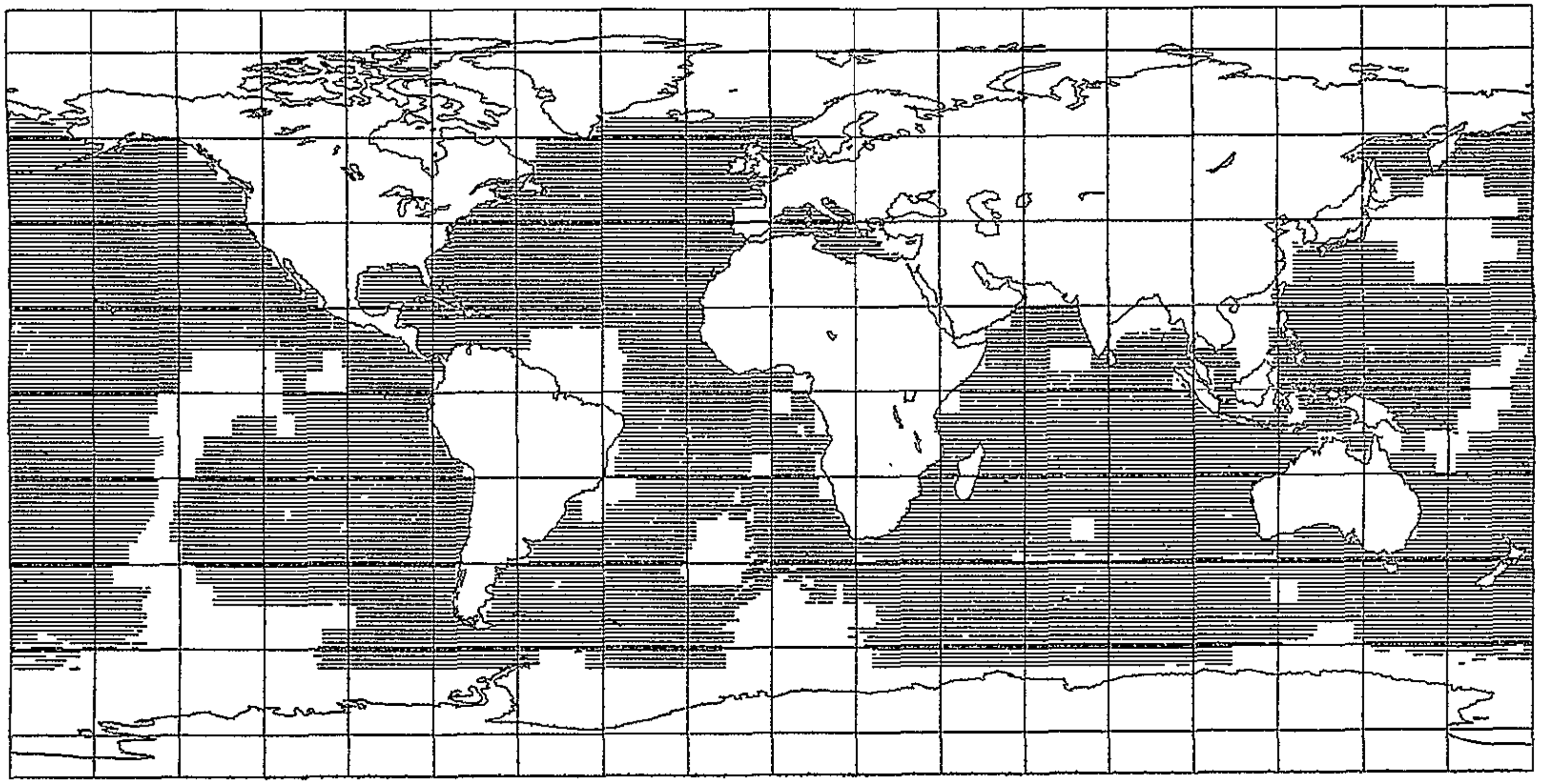

Figure 11. Location of 27466 $1^\circ \times 1^\circ$ Anomalies Derived from Geos-3 Altimeter Data Where the Accuracy is ± 15 mgals or Better.

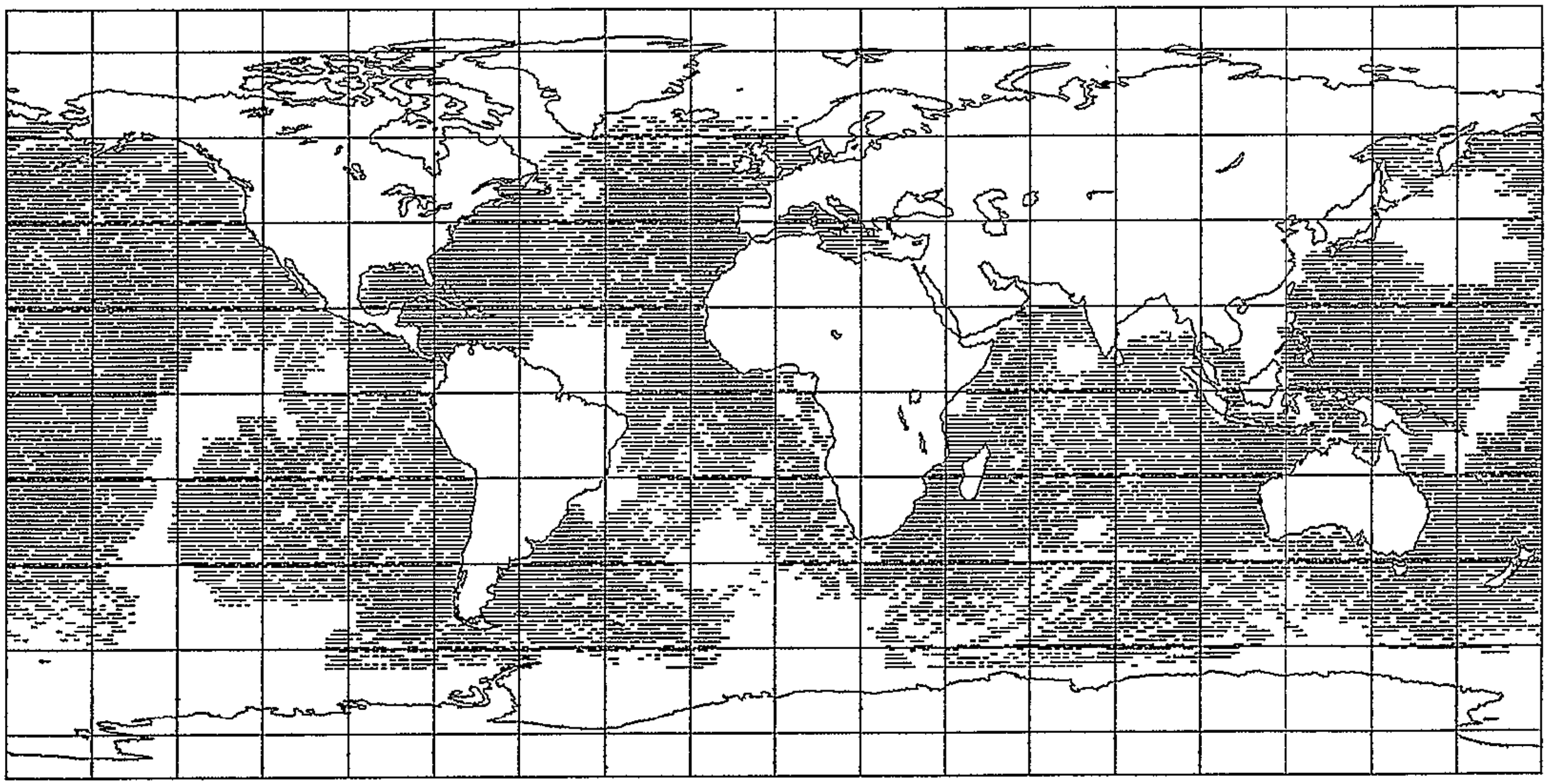

Figure 12. Location of 20599 1°x 1° Anomalies Derived from Geos-3 Altimeter Data where the Accuracy is ± 8 mgals or Better.

Table 14. Comparison of 5° Equal Area, and 1°x 1°, Altimeter Derived and Terrestrial Mean Free Air Anomalies.

Description	5° EA Value	1°x 1° Value
Mean Difference (GEM 9-Terr.)	0.3 mgals	—
Mean Difference (Alt. - Terr.)	0.7	0.5
RMS Difference (GEM 9 - Terr.)	±8.9	23.4
RMS Difference (Alt. - Terr.)	6.8	11.8
RMS Terrestrial Accuracy	4.8	10.9
RMS Altimeter Accuracy	2.7	7.8
RMS Terrestrial Anomaly	15.2	27.7
Maximum Difference	35.9	63.8
Number of Differences > $\lvert y \rvert$ mgals	10 *	7 †
Number of blocks compared	767	10086

* y = 20, † y = 40

We see that the altimeter anomalies have a better agreement with the terrestrial anomalies than the GEM 9 anomalies (computed from potential coefficients to degree 20) as would be expected. The average accuracy of the 5° altimeter anomalies is 3 mgals while it is 4 mgals for the terrestrial data used. The RMS difference between the 5° terrestrial and altimeter anomalies of 6.8 mgals is somewhat greater than would be expected if the terrestrial and altimeter accuracies were correct. We finally note a very small (0.7 mgal) systematic difference between the terrestrial and altimeter anomalies.

The 1°x 1° anomaly comparisons show a 11.8 mgals RMS differences between the altimeter and terrestrial data with only a 0.5 mgals systematic difference. This RMS difference is somewhat smaller than would be expected from the average accuracy estimates of the two data types which is about 11 mgals for the terrestrial data and 8 mgals for the altimeter values.

The 1°x 1° mean geoid undulations estimated from the altimeter data were compared to the GEM 9 undulations (computed to degree 20) where we found a mean difference of 0.0 meters and a root mean square difference of ±2.7 m. This difference is consistent with the expected value of ±3.2 meters.

Estimation in Small Areas

The preceeding computations have described the estimation of mean anomalies and mean undulations. It is of interest to examine the values to be obtained on the scale smaller than the 1° x 1° anomalies considered in this report. One attempt at this is described in Rapp (1978a, 1979) where point anomaly profiles were constructed across the Bonin Trench and around a sea mount in the Gulf of Alaska. In the case of the trench we saw an anomaly change of 443 mgals in

118 km. This large change indicated that there was high frequency anomaly information within the altimeter derived undulations. However we did not have at that time ship gravity data to compare with our altimeter derived anomalies.

Recently Detrick and Watts (1979) have described some investigations near the Ninety-East Ridge. These studies pointed out a region of available ship gravity data with bathymetric data that would provide a useful test area.

We first constructed an altimeter geoid in the area of the ridge which is shown as Figure 13. This map shows the undulation contours at 1 m intervals with the altimeter tracks plotted. In addition the 4000 m depth contour taken fromSclater and Fisher (1974) has been plotted to aide in the identification of the ridge crest. The depth of the actual crest varies approximately between 2000 m and 3500 meters.

This map has been prepared using the altimeter data of the first adjustment using a prediction interval of $0\overset{\circ}{.}5 \times 0\overset{\circ}{.}5$. In addition a few bad data points (newly discovered) were removed from the data set. Consequently this geoid will differ somewhat from that global representation described earlier.

For much of the geoid map there seems to be no specific association with the ridge although some dependence may be seen in the more southern parts.

To specifically test the anomaly prediction process ship data was obtained from Watts (private communication). The tracks obtained corresponded to some of the profiles described in Detrick and Watts (1979).

The point anomalies were predicted from the altimeter data at the same points as the existing ship gravity measurements. The prediction was carried out using one or two data selections and matrix inversions per profile. The results of these predictions are shown in Figures 14 and 15 where we have plotted the altimeter derived geoid, the altimeter derived anomalies, the ship determined anomalies and the measured bathymetry.

The profile shown in Figure 14 corresponds to the data used to obtain profile 90 E-9 in Detrick and Watts (1979). The starting (S) and ending (E) coordinates are: $\varphi_S = -3\overset{\circ}{.}19$, $\lambda_S = 85\overset{\circ}{.}115$, $\varphi_E = -4\overset{\circ}{.}00$, $\lambda_E = 93\overset{\circ}{.}515$. The profile shown in Figure 15 corresponds to the data used to obtain profile 90 E-12 in Detrick and Watts (1979). The starting and ending coordinates are: $\varphi_S = -16\overset{\circ}{.}755$ $\lambda_S = 8\overset{\circ}{.}3225$, $\varphi_E = -17\overset{\circ}{.}507$, $\lambda_E = 91\overset{\circ}{.}874$.

We can see that the altimeter anomalies follow quite closely the ship data except for the high frequency components. There is a clear correlation of the altimeter derived anomalies with the bathymetry. On the other hand the geoid seems to vary quite smoothly across the ridge, showing a small bump at the ridge crest.

Figure 13.

Altimeter Geoid in the Area of the Ninety-East Ridge Showing Location of 4000m Depth and Altimeter Tracks. Contour Interval = 1 m.

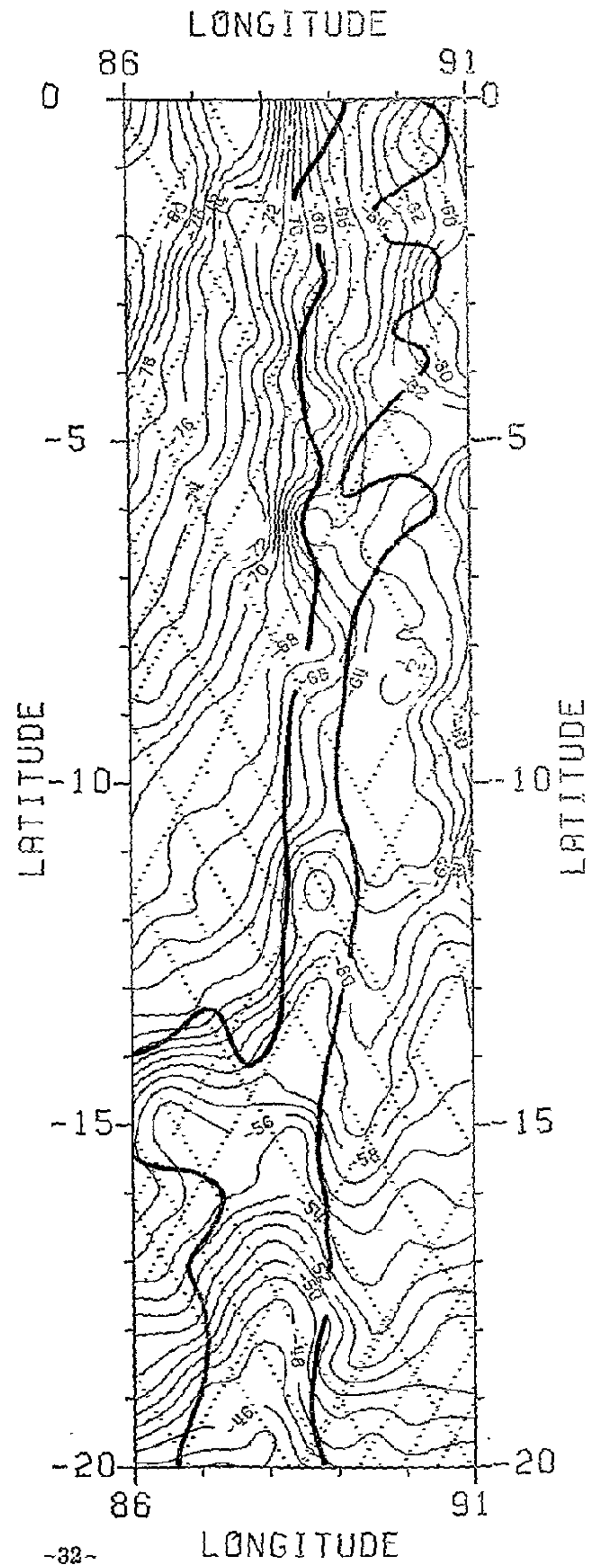

FIGURE 14. UNDULATION, ANOMALY, AND BATHYMETRY ACROSS 90 EAST RIDGE AT $\phi \sim -3.6°$

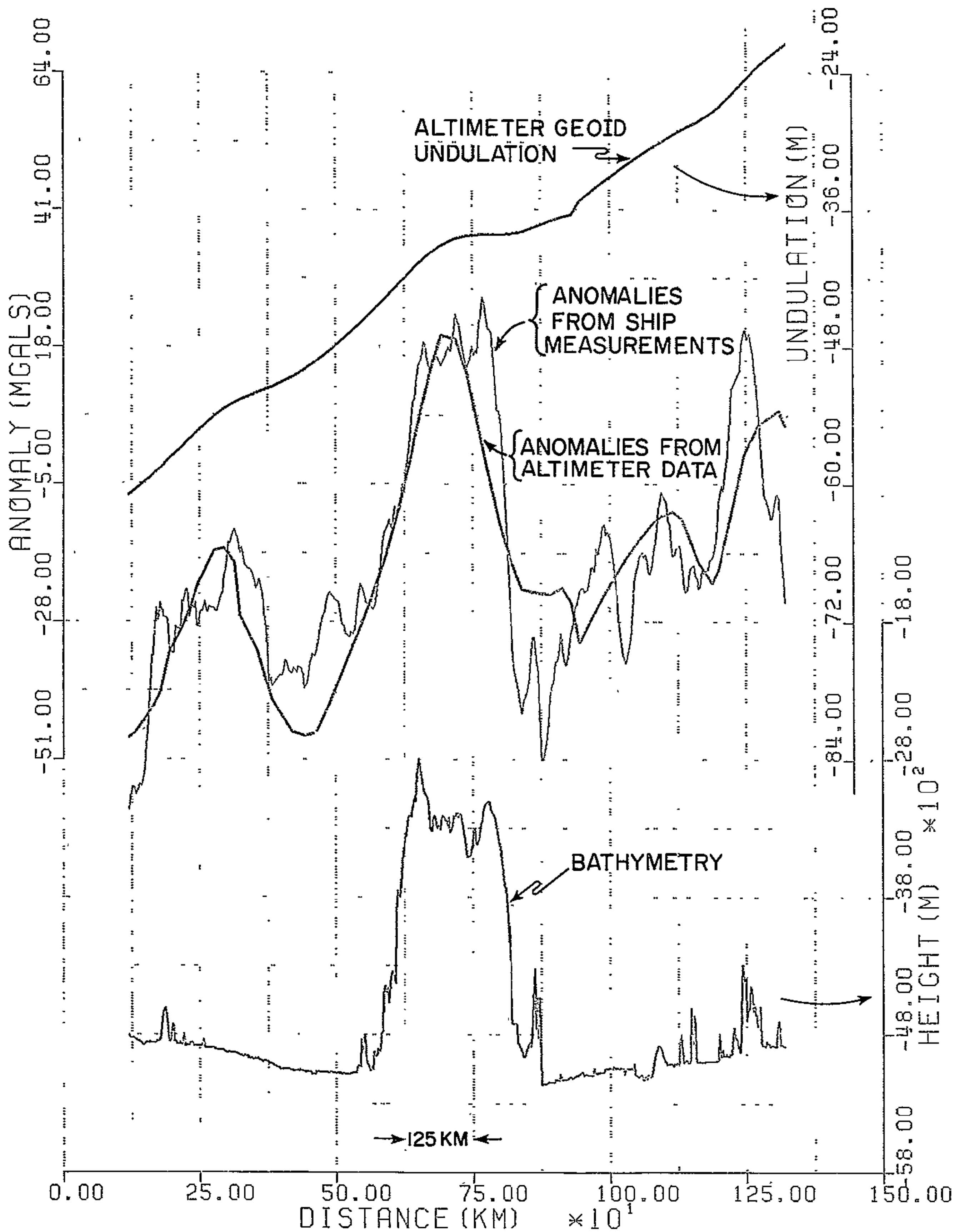

FIGURE 15. UNDULATION, ANOMALY, AND BATHYMETRY ACROSS 90 EAST RIDGE AT $\phi \sim -17°$

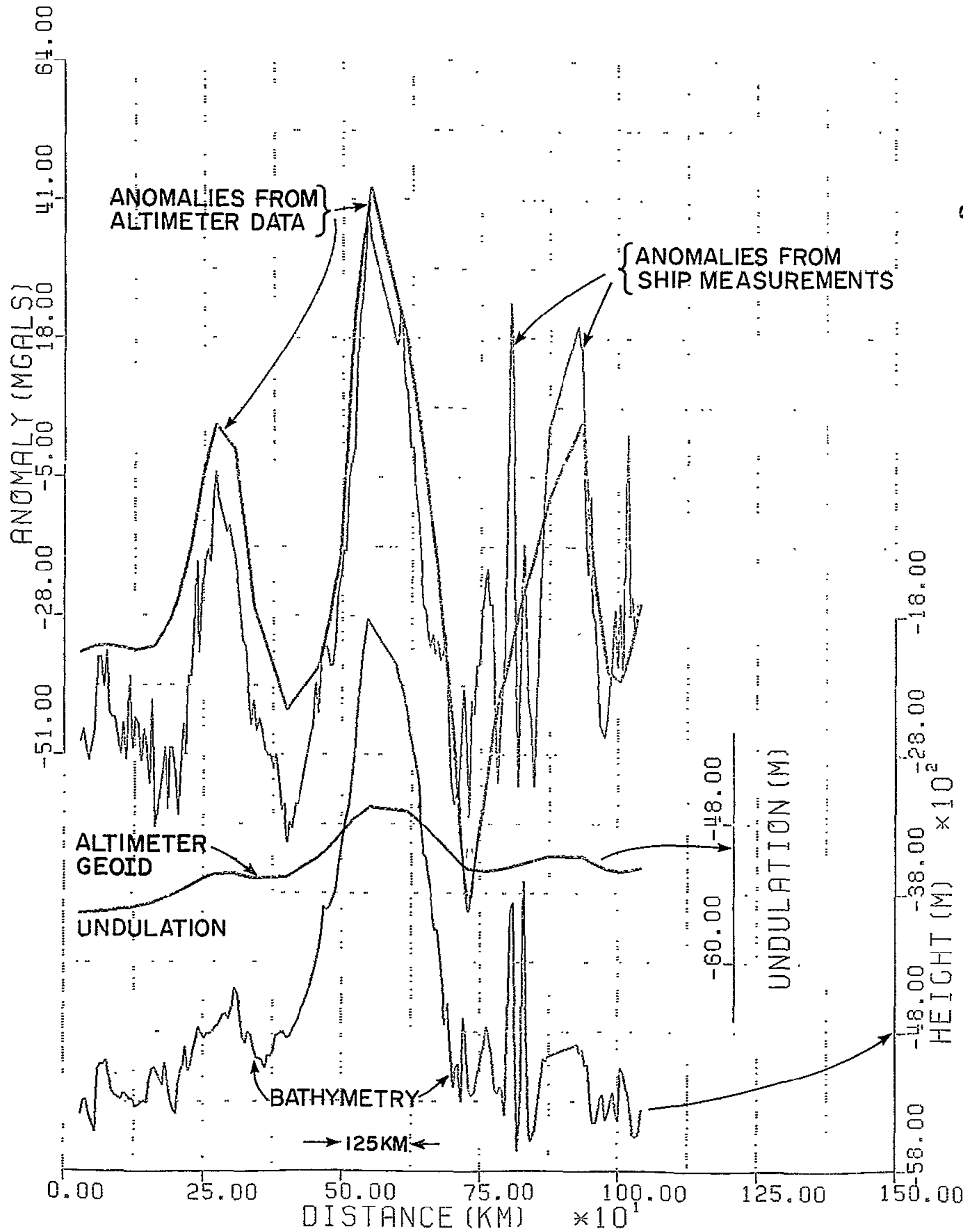

ORIGINAL PAGE IS OF POOR QUALITY

The RMS differences between the ship data and the altimeter data for the profile shown in Figures 14 and 15 was 12 mgals and 20 mgals respectively. The average predicted accuracy was 26 mgals. If the ship data is filtered to remove the high frequency components this agreement between the ship and the altimeter derived anomalies improves. For example, Eren (1979, private communication) has shown that if the components below a wavelength of 100 km are filtered out, the RMS differences for both profiles shown in Figure 14 and 15 become ±11 mgals.

There seems to be two conclusions to be reached from these specific studies. First the altimeter derived anomalies agree quite well with the ship data considering the accuracy of both data types. The altimeter anomalies seem to reflect the general bathymetry but they do not reflect the high frequency information seen by the ship measurements. More detailed analysis is needed to assess the accuracy of both data types by wavelength. In addition we need to look at the use of more detailed altimeter data as opposed to using from averages which represent an immediate averaging and loss of high frequency information.

Second we see that the geoid undulations only slightly reflect the variations going over the ridge. The significant variation is seen much more in examining the anomaly data.

Summary and Conclusions

This report has described the processing and analysis of Geos-3 data released for general use by March 1978. The data was edited and adjusted to remove bad data and to remove orbit and altimeter bias terms. The adjustment was carried out first in a primary set involving 700 arcs chosen for their global distribution, and 4 regional adjustments. The crossover discrepancies after the adjustment averaged about ±55 cm.

The resultant data was used to prepare a global sea surface map (or approximately the geoid) with accuracy estimates. Comparisons of these maps with similar data produced using precise orbits indicated random differences on the order of 1 meter with a systematic difference implying an equatorial radius of 6378137 meters. Computations were also done to investigate the accuracy of the altimeter geoid by wavelength. Comparisons with the undulation implied by the GEM 9 potential coefficients showed differences of about 75 cm at 5 wavelengths from 13010 km to 2602 km.

Several investigations were also carried out to improve our mean anomaly and mean undulation computation procedures. Specifically we considered the use of the smoothing operator in the series covariance expressions instead of numerical integration procedures for mean covariance computations. Although the procedure could save some computer time without any significant loss of accuracy, the original numerical integration procedure was retained for logistical reasons.

We also considered the correlation between various $1^\circ \times 1^\circ$ predictions within a 5° equal area block. We found that the average correlation coefficient between adjacent blocks was about 0.2 so that the blocks could be considered to have been determined independently.

The altimeter data was then used to extend our 5° and $1^\circ \times 1^\circ$ mean anomaly and undulation computation. For some unknown reason the data from our original adjustment in 1977 gave somewhat better anomalies than the new adjustment. Consequently in those geographic areas where the old adjustment data was adequate we used that data for anomaly estimation. In the other areas the new adjustment data was used. A total of 29479 $1^\circ \times 1^\circ$ blocks and 957 5° equal area blocks were estimated. Of these $1^\circ \times 1^\circ$ values 27466 had predicted standard deviations of ± 15 mgals or better. Comparisons were made with the terrestrial anomaly data where we found differences on the order of ± 12 mgals for the $1^\circ \times 1^\circ$ data and ± 7 mgals for the 5° data. A good part of this difference is due to the errors in the terrestrial anomaly field.

The anomaly and undulation predictions were done with a global covariance function referred to a degree 20 reference field. Additional tests were carried out with a different global covariance function and a local covariance function derived for special areas. No significant changes were seen in the predictions from the two global field models. Root mean square differences on the order of 3 mgals were found between the global and local covariance function but no significant improvement in the prediction process was seen based on comparisons with actual data. We did see changes in the predicted standard deviations up to 65% when using the local model instead of the global covariance model. The difficulty in applying a local model lies in a need for an adequate knowledge of the residual anomaly and undulation field in the area.

Point anomaly and undulation values were also computed along ship tracks that crossed the Ninety-East Ridge. The resultant anomaly values were compared to ship data where root mean square differences were 12 and 20 mgals for the two tracks considered. Plots of this data with the bathymetric indicate the correlation of the altimeter anomalies with the bathymetry on a regional basis as opposed to a more local correlation seen in the ship gravity data. Part of this difference may be due to our use of altimeter averages over 14 to 20 km swaths. However, we clearly can see the potential for improved knowledge of the anomaly field in small areas using the altimeter data.

What additional things need to be done? First the data needs to be reexamined to try to delete some additional bad data that has shown up. We should try to get additional data to fill in those areas for which data is non-existent or sparse. Then a readjustment could be done and the anomalies and undulations computed using localized covariance functions. One should also examine the use of non-frame averages going back, perhaps to the original data, or 1 second averages. The information, by wavelength, in the altimeter data should be studied to examine the accuracy of our anomaly and undulation results. And, of course, attempts have been made, and could continue to define sea surface topography effects.

Finally, it sould be clear that this Geos-3 altimeter data has enabled a significant improvement in our knowledge of the earth's gravity field. It's use in local areas and in global computations has added significantly to geodetic and geophysical research. This data and Seasat-1 data will provide a data source for additional research into the gravity field at sea and indirectly on a global basis.

References

Anderle, R., Earth's Semi-Major Axis, unpublished memo dated 1 May 1979.

Brace, K. Preliminary Ocean-Area Geoid from Geos-3 Satellite Radar Altimetry, Defense Mapping Agency Aerospace Center, St. Louis, 1977.

Detrick, R., and A. Watts, An Analysis of Isostasy in the World's Oceans, 3. Aseismic Ridges, J. Geophys. Res., (in press) 1979.

Heiskanen, W., and H. Moritz, Physical Geodesy, W.H. Freeman and Co., San Francisco, 1967.

IAG, Geodetic Reference System 1967, Special Publication of the Bulletin Geodesique, International Association of Geodesy, 1971.

Jekeli, C., An Investigation of Two Models for the Degree Variances of Global Covariance Functions, Dept. of Geodetic Science Report No. 275, The Ohio State University, Columbus, 77p.,1978.

Jordan, S., Self-Consistent Statistical Models for the Gravity Anomaly, Vertical Deflections, and Undulation of the Geoid, J. Geophys. Res., 77, 20, 3660-3670, 1972.

Kearsley, W., The Prediction and Mapping of Geoidal Undulations from Geos-3 Altimetry, Dept. of Geodetic Science Report No. 267, The Ohio State University, Columbus, 68p., 1977.

Lerch, F., S. Klosko, R. Laubscher, and C. Wagner, Gravity Model Improvement Using Geos-3 (GEM 9 and 10), NASA Document X-921-77-246, Goddard Space Flight Center, Greenbelt, Maryland, 1977.

Marsh, J., T. Martin, S. McCarthy, and P. Chovitz, Mean Sea Surface Computation using Geos-3 Altimeter Data, paper presented at the International Symposium on Interaction of Marine Geodesy and Ocean Dynamics, Miami, October 1978. (Washington Analytic Services Center, 6801 Kenilworth Ave., Riverdale, Maryland.)

Meissl, P., A Study of Covariance Functions Related to the Earth's Disturbing Potential, Dept. of Geodetic Science Report No. 151, The Ohio State University, Columbus, 87 p. 1971.

Moritz, H., Advanced Least Squares Methods, Dept. of Geodetic Science Report No. 175, The Ohio State University, Columbus, 133p. 1972.

Moritz, H., Least-Squares Collocation, Reviews of Geophysics and Space Physics, Vol. 16, No. 3, 421-430, 1978.

Rapp, R. H., The Relationship Between Mean Anomaly Block Sizes and Spherical Harmonic Representations, J. Geophys. Res., 82, 33, 5360-5364, 1977b.

Rapp, R. H., Mean Gravity Anomalies and Sea Surface Heights Derived from Geos-3 Altimeter Data, Dept. of Geodetic Science Report No. 268, The Ohio State University, Columbus, 120 p., 1977a.

Rapp, R.H., Gravity Anomaly and Geoid Undulation Results in Local Areas from Geos-3 Altimeter Data, paper presented at the 1978 Spring Meeting of the American Geophysical Union, Miami Beach, 1978a.

Rapp, R. H., A Combined Terrestrial-Altimeter $1^\circ \times 1^\circ$ Mean Gravity Anomaly Field, paper presented at the Eighth Meeting of the International Gravtty Commission, Paris, September 1978b.

Rapp, R. H., Geos-3 Data Processing for the Recovery of Geoid Undulations and Gravity Anomalies, J. Geophys. Res., 84, 1979.

Rummel, R., and R. H. Rapp, Undulation and Anomaly Estimation Using Geos-3 Altimeter Data Without Precise Satellite Orbits, Bulletin Geodesique, No. 51, 73-88, 1977.

Schwarz, K-P., Geodetic Accuracies Obtainable from Measurements of First and Second Order Gravitational Gradients, Dept. of Geodetic Science Report No. 242, The Ohio State University, 56 p., 1976.

Sclater, J. G., and R. L. Fisher, Evolution of the East Central Indian Ocean, With Emphasis on the Tectonic Setting of the Ninety-East Ridge, Geol. Soc. Am. Bull. 85, 683-702, 1974.

Sunkel, H., A General Surface Representation Module Designed for Geodesy, Dept. of Geodetic Science Report, The Ohio State University, Columbus, 1979.

Tscherning, C., and R. H. Rapp, Closed Covariance Expressions for Gravity Anomalies, Geoid Undulations, and Deflections of the Vertical Implied by Anomaly Degree Variance Models, Dept. of Geodetic Science Report No. 208, The Ohio State University, Columbus, 89 p.,1974.

Appendix

This appendix contains a listing of the 5° equal area free-air anomalies and undulations as derived from Geos-3 altimeter data. These values refer to an ellipsoid whose flattening is 1/298.257 and whose equatorial radius is theoretically unknown, being actually the equatorial radius of the general terrestrial ellipsoid.

SEQ	LAT		LONG		ANOM	S.D.	UND	S.D.
79	65	60	11	0	11.4	3.4	44.2	0.5
96	65	60	196	185	8.6	2.7	8.8	0.1
109	65	60	338	327	33.5	2.6	62.1	0.1
111	65	60	0	349	17.7	2.5	54.3	0.1
127	60	55	148	138	10.4	3.1	16.8	0.3
129	60	55	166	157	21.7	3.3	15.9	0.4
131	60	55	185	175	-10.2	2.5	2.9	0.1
133	60	55	203	194	27.5	2.7	15.3	0.2
135	60	55	222	212	14.0	2.7	8.3	0.1
146	60	55	323	314	21.0	2.5	45.7	0.1
148	60	55	342	332	21.4	2.5	67.9	0.1
150	60	55	0	351	20.5	2.6	54.2	0.2
168	55	50	147	139	7.7	2.9	19.7	0.2
170	55	50	164	155	13.7	2.7	16.2	0.2
172	55	50	180	172	-5.0	2.4	0.8	0.1
174	55	50	196	188	12.9	2.5	7.6	0.1
176	55	50	213	205	23.6	2.5	7.2	0.1
178	55	50	229	221	-2.7	2.6	-9.4	0.1
189	55	50	319	311	14.0	2.8	34.7	0.1
191	55	50	335	327	26.1	2.4	61.0	0.1
193	55	50	352	344	21.9	2.5	59.0	0.1
215	50	45	154	147	22.8	2.5	20.2	0.1
219	50	45	184	176	10.5	2.5	-2.7	0.1
221	50	45	198	191	14.0	2.4	2.9	0.1
223	50	45	213	206	3.0	2.5	-5.8	0.1
225	50	45	228	220	-14.8	2.5	-23.2	0.1
235	50	45	301	294	-12.3	2.8	-16.9	0.1
237	50	45	316	309	19.9	2.7	25.7	0.1
239	50	45	331	323	28.5	2.5	64.4	0.1
241	50	45	345	338	23.6	2.4	60.6	0.1
243	50	45	0	353	7.1	2.8	50.4	0.2
245	45	40	14	7	16.7	3.1	47.2	0.3
270	45	40	183	177	-11.6	2.5	-8.8	0.1
272	45	40	197	190	-3.5	2.5	-7.3	0.1
274	45	40	211	204	-3.4	2.5	-13.7	0.1
276	45	40	224	217	-12.2	2.5	-26.5	0.1
278	45	40	238	231	-7.6	3.0	-28.3	0.4
287	45	40	299	292	-6.6	2.5	-24.7	0.1
289	45	40	312	306	5.8	2.5	4.9	0.1
291	45	40	326	319	17.7	2.4	42.7	0.1
293	45	40	340	333	31.0	2.4	60.3	0.1
295	45	40	353	346	11.5	2.7	52.7	0.2
298	40	35	13	6	17.2	2.9	50.5	0.3
300	40	35	25	19	-7.3	2.9	30.0	0.2
325	40	35	183	177	-13.3	2.5	-11.5	0.1
327	40	35	196	189	-13.3	2.5	-13.9	0.1
329	40	35	208	202	-8.8	2.5	-16.2	0.1
331	40	35	221	215	-21.1	2.5	-29.7	0.1
333	40	35	234	227	-24.1	2.5	-44.0	0.1
342	40	35	291	284	-23.3	2.7	-45.9	0.1
344	40	35	303	297	-13.3	2.5	-27.7	0.1
346	40	35	316	309	-4.3	2.6	5.9	0.1
348	40	35	328	322	29.1	2.4	44.2	0.1
350	40	35	341	335	12.3	2.4	48.9	0.1

SEQ	LAT		LONG		ANOM	S.D.	UND	S.D.
95	65	60	185	175	-2.3	2.9	4.5	0.2
108	65	60	327	316	18.5	2.9	49.7	0.3
110	65	60	349	338	27.3	2.8	61.8	0.2
112	60	55	9	0	4.1	2.7	44.2	0.1
128	60	55	157	148	15.3	2.8	17.9	0.2
130	60	55	175	166	-2.9	2.5	5.5	0.1
132	60	55	194	185	13.9	2.5	10.5	0.1
134	60	55	212	203	15.0	2.9	12.4	0.2
145	60	55	314	305	7.5	2.6	24.8	0.1
147	60	55	332	323	34.7	2.5	59.9	0.1
149	60	55	351	342	10.8	2.5	57.9	0.1
151	55	50	8	0	-3.2	3.3	44.5	0.5
169	55	50	155	147	9.7	2.5	19.4	0.1
171	55	50	172	164	3.2	2.5	4.3	0.1
173	55	50	188	180	-14.5	2.4	1.1	0.1
175	55	50	205	196	20.2	2.5	11.0	0.1
177	55	50	221	213	8.8	2.5	-1.1	0.1
188	55	50	311	303	8.0	2.7	14.3	0.1
190	55	50	327	319	27.6	2.5	52.7	0.1
192	55	50	344	335	18.4	2.5	68.2	0.1
194	55	50	0	352	15.4	2.9	53.3	0.3
218	50	45	176	169	-4.4	2.5	-3.5	0.1
220	50	45	191	184	18.0	2.4	1.1	0.1
222	50	45	206	198	10.6	2.5	0.0	0.1
224	50	45	220	213	-4.2	2.5	-13.2	0.1
226	50	45	235	228	-6.7	2.7	-21.7	0.1
236	50	45	309	301	2.7	2.8	3.4	0.2
238	50	45	323	316	13.2	2.5	40.8	0.1
240	50	45	338	331	36.7	2.4	64.5	0.1
242	50	45	353	345	10.4	2.5	62.0	0.1
244	45	40	7	0	15.4	3.6	49.6	0.6
246	45	40	20	14	22.9	3.4	37.9	0.4
271	45	40	190	183	-9.3	2.5	-8.6	0.1
273	45	40	204	197	-2.4	2.5	-9.2	0.1
275	45	40	217	211	-5.9	2.5	-17.1	0.1
277	45	40	231	224	-12.2	2.5	-29.8	0.1
286	45	40	292	285	0.6	3.9	-29.2	0.8
288	45	40	306	299	-18.4	2.5	-15.3	0.1
290	45	40	319	312	4.9	2.7	23.4	0.1
292	45	40	333	326	36.7	2.5	58.6	0.1
294	45	40	346	340	11.3	2.4	47.3	0.1
297	40	35	6	0	12.6	3.0	46.3	0.3
299	40	35	19	13	9.2	2.5	37.5	0.1
324	40	35	177	171	-12.5	2.5	-11.1	0.1
326	40	35	189	183	-14.4	2.4	-12.1	0.1
328	40	35	202	196	-9.7	2.5	-13.2	0.1
330	40	35	215	208	-14.5	2.5	-25.6	0.1
332	40	35	227	221	-21.9	2.5	-34.8	0.1
334	40	35	240	234	-11.9	3.3	-34.7	0.5
343	40	35	297	291	-23.4	2.4	-36.8	0.1
345	40	35	309	303	-10.9	2.5	-14.7	0.1
347	40	35	322	316	10.4	2.4	26.3	0.1
349	40	35	335	328	38.7	2.5	61.1	0.1
351	40	35	347	341	12.4	2.4	48.4	0.1

SEQ	LAT		LONG		ANOM	S.D.	UND	S.D.
352	40	35	354	347	17.7	2.9	58.1	0.3
357	35	30	24	18	6.5	3.7	26.1	0.6
375	35	30	130	124	17.0	3.0	25.8	0.2
377	35	30	142	136	22.5	2.6	36.1	0.1
384	35	30	183	177	-8.5	2.5	-8.3	0.1
386	35	30	195	189	-12.1	2.5	-9.3	0.1
388	35	30	207	201	-6.6	2.5	-13.4	0.1
390	35	30	218	212	-9.8	2.5	-23.7	0.1
392	35	30	230	224	-14.1	2.5	-36.4	0.1
394	35	30	242	236	-13.9	2.6	-39.5	0.1
402	35	30	289	283	-32.5	2.5	-45.8	0.1
404	35	30	301	295	-8.3	2.5	-36.4	0.1
406	35	30	313	307	-6.6	2.5	-11.7	0.1
408	35	30	325	319	24.1	2.5	27.6	0.1
410	35	30	336	330	5.6	2.5	36.7	0.1
412	35	30	348	342	12.7	2.4	43.3	0.1
437	30	25	129	124	18.6	2.5	23.1	0.1
439	30	25	141	135	20.5	2.5	40.4	0.1
441	30	25	152	146	2.4	2.5	27.2	0.1
446	30	25	180	174	-9.0	2.5	-4.2	0.1
448	30	25	191	186	5.5	2.5	0.4	0.1
450	30	25	203	197	6.7	2.5	-1.8	0.1
452	30	25	214	208	1.5	2.5	-13.5	0.1
454	30	25	225	219	-5.4	2.6	-27.9	0.1
456	30	25	236	231	-16.3	2.4	-35.7	0.1
458	30	25	248	242	-13.7	2.7	-39.4	0.1
463	30	25	276	270	-3.3	2.7	-26.1	0.1
465	30	25	287	281	-17.8	2.5	-39.8	0.1
467	30	25	298	293	-13.6	2.4	-38.1	0.1
469	30	25	309	304	-19.5	2.5	-26.7	0.1
471	30	25	321	315	9.8	2.5	5.0	0.1
473	30	25	332	326	5.5	2.5	23.3	0.1
475	30	25	343	338	8.6	2.5	28.3	0.1
501	25	20	124	118	3.9	3.0	23.6	0.3
503	25	20	134	129	9.1	2.5	37.2	0.1
505	25	20	145	140	14.6	2.5	43.1	0.1
507	25	20	156	150	3.4	2.5	34.7	0.1
509	25	20	167	161	-7.7	2.5	13.9	0.1
511	25	20	177	172	-9.0	2.5	2.3	0.1
513	25	20	188	183	-3.7	2.5	3.9	0.1
515	25	20	199	193	19.4	2.5	10.1	0.1
517	25	20	210	204	6.3	2.3	-3.9	0.1
519	25	20	220	215	-3.6	2.4	-19.4	0.1
521	25	20	231	226	-13.4	2.4	-36.8	0.1
523	25	20	242	236	-26.6	2.5	-53.5	0.1
525	25	20	253	247	-9.4	2.6	-39.8	0.1
529	25	20	274	269	6.6	2.6	-16.9	0.2
531	25	20	285	279	8.1	2.5	-31.1	0.1
533	25	20	296	290	-31.6	2.5	-60.5	0.1
535	25	20	306	301	-22.5	2.5	-42.4	0.1
537	25	20	317	312	-0.8	2.8	-14.4	0.1
539	25	20	328	322	-2.6	2.5	3.6	0.1
541	25	20	339	333	-1.5	2.5	23.2	0.1
557	20	15	63	57	-10.1	2.6	-53.3	0.1

SEQ	LAT		LONG		ANOM	S.D.	UND	S.D.
356	35	30	18	12	7.1	3.2	32.8	0.5
358	35	30	30	24	-14.6	3.7	19.2	0.4
376	35	30	136	130	12.1	2.6	32.6	0.1
378	35	30	148	142	-4.1	2.5	25.0	0.1
385	35	30	189	183	-10.6	2.5	-9.1	0.1
387	35	30	201	195	-7.4	2.4	-10.1	0.1
389	35	30	212	207	-5.2	2.5	-14.7	0.1
391	35	30	224	218	-9.1	2.5	-29.8	0.1
393	35	30	236	230	-15.0	2.5	-40.4	0.1
401	35	30	283	277	-3.9	3.6	-33.7	0.6
403	35	30	295	289	-23.9	2.5	-44.8	0.1
405	35	30	307	301	-18.1	2.5	-28.6	0.1
407	35	30	319	313	10.7	2.5	9.6	0.1
409	35	30	330	325	13.2	2.4	29.5	0.1
411	35	30	342	336	-2.6	2.4	37.4	0.1
413	35	30	354	348	14.6	3.4	45.7	0.6
438	30	25	135	129	-13.8	2.5	-2.7	0.1
440	30	25	146	141	6.9	2.4	29.3	0.1
445	30	25	174	169	-14.7	2.4	-3.7	0.1
447	30	25	186	180	-2.8	2.5	-2.3	0.1
449	30	25	197	191	9.2	2.5	1.5	0.1
451	30	25	208	203	-1.9	2.5	-6.6	0.1
453	30	25	219	214	1.1	2.4	-16.7	0.1
455	30	25	231	225	-12.0	2.5	-36.4	0.1
457	30	25	242	236	-18.0	2.5	-44.2	0.1
462	30	25	270	264	-12.0	2.9	-26.7	0.1
464	30	25	281	276	5.8	2.6	-21.8	0.2
466	30	25	293	287	-30.2	2.5	-49.2	0.1
468	30	25	304	298	-27.2	2.5	-42.8	0.1
470	30	25	315	309	-2.1	2.5	-13.4	0.1
472	30	25	326	321	2.5	2.5	12.4	0.1
474	30	25	338	332	-3.1	2.6	27.3	0.1
476	30	25	349	343	6.6	3.1	38.5	0.4
502	25	20	129	124	3.4	2.5	30.0	0.1
504	25	20	140	134	14.4	2.5	51.5	0.1
506	25	20	150	145	0.9	2.6	34.9	0.1
508	25	20	161	156	-3.0	2.5	19.3	0.1
510	25	20	172	167	-8.5	2.5	5.5	0.1
512	25	20	183	177	-9.8	2.6	1.8	0.1
514	25	20	193	188	7.2	2.5	7.9	0.1
516	25	20	204	199	22.3	2.4	6.4	0.1
518	25	20	215	210	0.9	2.4	-11.8	0.1
520	25	20	226	220	-8.9	2.5	-33.5	0.1
522	25	20	236	231	-16.2	2.5	-42.5	0.1
524	25	20	247	242	-19.3	2.5	-42.9	0.1
528	25	20	269	263	-20.7	2.6	-25.8	0.1
530	25	20	279	274	-5.4	2.4	-19.9	0.1
532	25	20	290	285	-32.5	2.6	-42.4	0.1
534	25	20	301	296	-24.1	2.4	-49.2	0.1
536	25	20	312	306	-19.7	2.5	-36.6	0.1
538	25	20	322	317	-5.8	2.6	-4.5	0.2
540	25	20	333	328	5.8	2.4	18.2	0.1
542	25	20	344	339	2.8	2.7	30.0	0.1
558	20	15	68	63	-11.9	2.5	-62.1	0.1

SEQ	LAT		LONG		ANOM	S.D.	UND	S.D.
559	20	15	73	68	-26.3	2.8	-72.5	0.1
570	20	15	130	125	13.1	2.5	42.0	0.1
572	20	15	141	136	13.9	2.4	49.4	0.1
574	20	15	151	146	-4.5	2.4	39.7	0.1
576	20	15	162	157	-1.2	2.4	26.2	0.1
578	20	15	172	167	1.0	2.5	15.3	0.1
580	20	15	183	177	-9.6	2.9	8.5	0.2
582	20	15	193	188	4.4	2.5	9.6	0.1
584	20	15	203	198	4.9	2.5	6.4	0.1
586	20	15	214	209	2.4	2.4	-6.7	0.1
588	20	15	224	219	-6.2	2.5	-22.5	0.1
590	20	15	235	230	-17.5	2.5	-40.2	0.1
592	20	15	245	240	-20.7	2.5	-44.0	0.1
594	20	15	256	250	-4.3	2.6	-31.0	0.1
598	20	15	277	271	13.2	2.9	-7.2	0.1
600	20	15	287	282	1.1	2.5	-20.7	0.1
602	20	15	297	292	-45.2	2.4	-46.1	0.1
604	20	15	308	303	-24.8	2.4	-42.4	0.1
606	20	15	318	313	-9.6	2.8	-20.5	0.2
608	20	15	329	323	-0.9	2.7	3.7	0.1
610	20	15	339	334	24.4	2.4	26.0	0.1
625	15	10	57	51	2.6	2.6	-47.9	0.1
627	15	10	67	62	-17.8	2.5	-69.9	0.1
629	15	10	77	72	-30.8	3.2	-89.5	0.5
632	15	10	93	87	-26.2	3.1	-80.5	0.3
638	15	10	123	118	28.4	2.8	46.6	0.1
640	15	10	134	129	9.9	2.4	54.1	0.1
642	15	10	144	139	-4.4	2.5	51.4	0.1
644	15	10	154	149	-3.1	2.5	42.4	0.1
646	15	10	165	159	-0.9	2.5	36.3	0.1
648	15	10	175	170	-4.3	3.0	18.1	0.2
650	15	10	185	180	-6.1	2.8	10.3	0.2
652	15	10	195	190	3.6	2.5	11.3	0.1
654	15	10	206	201	-2.7	2.5	4.8	0.1
656	15	10	216	211	2.0	2.4	-4.6	0.1
658	15	10	226	221	-2.1	2.5	-19.9	0.1
660	15	10	237	231	-21.0	2.6	-44.8	0.1
662	15	10	247	242	-18.6	2.7	-39.0	0.2
664	15	10	257	252	-1.3	2.6	-20.9	0.1
666	15	10	267	262	10.3	2.4	-5.3	0.1
668	15	10	278	273	30.9	3.5	6.0	0.5
670	15	10	288	283	-4.9	2.7	-12.4	0.2
672	15	10	298	293	-14.3	2.8	-33.1	0.1
678	15	10	329	324	-14.1	2.7	-3.1	0.1
680	15	10	339	334	-2.6	2.4	17.4	0.1
695	10	5	56	51	-29.9	2.5	-51.1	0.1
697	10	5	66	61	-17.1	2.5	-71.2	0.1
701	10	5	86	81	-42.2	2.3	-93.4	0.1
703	10	5	96	91	-16.6	2.5	-50.6	0.1
705	10	5	106	101	-0.4	2.7	-7.1	0.1
708	10	5	122	117	32.1	3.3	53.3	0.5
710	10	5	132	127	10.0	2.5	62.5	0.1
712	10	5	142	137	21.9	2.4	63.4	0.1
714	10	5	152	147	12.6	2.5	55.1	0.1

SEQ	LAT		LONG		ANOM	S.D.	UND	S.D.
569	20	15	125	120	16.0	2.9	36.4	0.2
571	20	15	136	130	5.8	2.5	53.8	0.1
573	20	15	146	141	31.2	2.5	50.7	0.1
575	20	15	157	151	6.3	2.5	41.5	0.1
577	20	15	167	162	2.0	2.5	20.8	0.1
579	20	15	177	172	-6.3	2.5	10.0	0.1
581	20	15	188	183	-1.3	2.6	8.0	0.1
583	20	15	198	193	0.3	2.5	8.3	0.1
585	20	15	209	203	9.1	2.5	1.2	0.1
587	20	15	219	214	-2.8	2.4	-14.3	0.1
589	20	15	230	224	-15.1	2.7	-38.2	0.1
591	20	15	240	235	-20.4	2.6	-44.3	0.1
593	20	15	250	245	-12.4	2.6	-37.0	0.1
595	20	15	261	256	9.4	4.5	-14.3	0.9
599	20	15	282	277	12.2	2.5	-10.2	0.1
601	20	15	292	287	-4.7	2.5	-33.9	0.1
603	20	15	303	297	-46.1	2.5	-58.1	0.1
605	20	15	313	308	-17.1	2.5	-32.6	0.1
607	20	15	323	318	-13.1	2.5	-11.3	0.1
609	20	15	334	329	14.0	2.5	17.2	0.1
611	20	15	344	339	6.5	2.8	28.8	0.1
626	15	10	62	57	-4.0	2.5	-53.9	0.1
628	15	10	72	67	-30.4	2.6	-83.5	0.1
631	15	10	87	82	-44.0	3.6	-86.9	0.6
633	15	10	98	93	-13.8	2.9	-46.8	0.2
639	15	10	129	123	29.3	2.6	64.2	0.1
641	15	10	139	134	11.8	2.4	55.1	0.1
643	15	10	149	144	-10.8	2.5	45.4	0.1
645	15	10	159	154	-3.4	2.5	36.1	0.1
647	15	10	170	165	0.0	2.5	24.3	0.1
649	15	10	180	175	-6.1	3.0	13.0	0.3
651	15	10	190	185	-3.6	2.6	10.0	0.1
653	15	10	201	195	1.3	2.6	11.3	0.1
655	15	10	211	206	-2.1	2.5	0.3	0.1
657	15	10	221	216	4.2	2.5	-11.0	0.1
659	15	10	231	226	-9.6	2.5	-29.2	0.1
661	15	10	242	237	-21.5	2.5	-41.5	0.1
663	15	10	252	247	-11.7	2.6	-31.3	0.1
665	15	10	262	257	12.4	2.7	-10.8	0.1
667	15	10	273	267	17.2	2.9	-0.1	0.2
669	15	10	283	278	7.1	2.4	-1.1	0.1
671	15	10	293	288	-19.7	2.9	-24.7	0.2
673	15	10	303	298	-37.1	2.5	-43.8	0.1
679	15	10	334	329	-4.6	2.5	8.6	0.1
681	15	10	345	339	8.8	2.8	31.2	0.2
696	10	5	61	56	0.1	2.5	-55.7	0.1
700	10	5	81	76	-36.2	3.0	-99.2	0.2
702	10	5	91	86	-9.2	2.5	-70.8	0.1
704	10	5	101	96	16.9	2.8	-23.2	0.2
706	10	5	112	106	13.0	3.3	18.8	0.5
709	10	5	127	122	41.1	2.5	64.2	0.2
711	10	5	137	132	20.0	2.5	64.4	0.1
713	10	5	147	142	19.3	2.4	60.3	0.1
715	10	5	157	152	8.6	2.5	48.8	0.1

SEQ	LAT		LONG		ANOM	S.D.	UND	S.D.	SEQ	LAT		LONG		ANOM	S.D.	UND	S.D.
716	10	5	162	157	7.3	2.4	42.0	0.1	717	10	5	167	162	-5.2	2.5	32.7	0.1
718	10	5	172	167	1.2	2.8	27.3	0.1	720	10	5	183	177	-6.5	3.0	19.0	0.3
721	10	5	188	183	-10.7	2.6	11.5	0.1	722	10	5	193	188	-4.4	2.5	11.8	0.1
723	10	5	198	193	4.9	2.5	13.9	0.1	724	10	5	203	198	10.8	2.5	13.9	0.1
725	10	5	208	203	12.0	2.5	10.7	0.1	726	10	5	213	208	8.1	2.4	5.5	0.1
727	10	5	218	213	4.2	2.5	-0.9	0.1	728	10	5	223	218	1.7	2.6	-8.5	0.1
733	10	5	248	243	-12.8	2.6	-32.1	0.1	734	10	5	254	248	-8.9	2.7	-30.3	0.1
736	10	5	264	259	5.2	2.6	-9.3	0.1	737	10	5	269	264	8.8	2.4	-2.9	0.1
738	10	5	274	269	15.6	2.4	3.9	0.1	739	10	5	279	274	30.6	2.5	11.4	0.1
740	10	5	284	279	41.1	2.8	13.1	0.2	749	10	5	330	325	6.0	2.6	1.3	0.2
750	10	5	335	330	4.3	2.4	9.6	0.1	751	10	5	340	335	7.1	2.4	16.8	0.1
752	10	5	345	340	1.8	2.4	22.1	0.1	753	10	5	350	345	24.1	3.4	30.6	0.6
756	5	0	5	0	-4.7	2.7	18.6	0.1	765	5	0	50	45	-27.9	3.0	-43.1	0.3
766	5	0	55	50	-19.3	2.5	-50.6	0.1	767	5	0	60	55	-14.9	2.5	-57.0	0.1
768	5	0	65	60	-17.3	2.5	-68.5	0.1	769	5	0	70	65	-27.5	2.9	-83.2	0.2
770	5	0	75	70	-34.1	2.9	-95.3	0.3	771	5	0	80	75	-47.9	2.5	-102.5	0.1
772	5	0	85	80	-52.4	2.5	-98.3	0.1	773	5	0	90	85	-24.6	2.5	-76.1	0.1
774	5	0	95	90	0.2	2.5	-49.2	0.1	777	5	0	110	105	24.8	2.7	19.9	0.1
780	5	0	125	120	44.0	2.6	63.5	0.1	781	5	0	130	125	34.3	2.5	66.5	0.1
782	5	0	135	130	37.9	2.5	72.9	0.1	783	5	0	140	135	24.7	2.5	70.7	0.1
784	5	0	145	140	19.2	2.4	68.5	0.1	785	5	0	150	145	12.3	2.4	63.4	0.1
786	5	0	155	150	3.3	2.5	56.7	0.1	787	5	0	160	155	13.0	2.5	52.9	0.1
788	5	0	165	160	6.5	2.5	43.5	0.1	791	5	0	180	175	-6.8	2.7	21.3	0.2
792	5	0	185	180	-2.6	2.5	17.8	0.1	793	5	0	190	185	-4.1	2.4	14.8	0.1
794	5	0	195	190	-1.8	2.5	14.4	0.1	795	5	0	200	195	7.0	2.5	16.0	0.1
796	5	0	205	200	20.3	2.5	17.6	0.1	797	5	0	210	205	17.6	2.4	14.3	0.1
798	5	0	215	210	13.9	2.4	9.3	0.1	799	5	0	220	215	11.8	3.0	2.7	0.2
805	5	0	250	245	-6.3	2.5	-23.9	0.1	808	5	0	265	260	-0.8	2.6	-10.3	0.1
809	5	0	270	265	3.4	2.4	-4.7	0.1	810	5	0	275	270	4.7	2.4	1.7	0.1
811	5	0	280	275	10.0	2.6	9.5	0.1	821	5	0	330	325	13.3	2.5	1.9	0.1
822	5	0	335	330	10.7	2.5	9.5	0.1	823	5	0	340	335	5.0	2.4	13.7	0.1
824	5	0	345	340	-3.7	2.4	16.8	0.1	825	5	0	350	345	-1.7	2.4	21.1	0.1
826	5	0	355	350	-4.3	2.7	22.0	0.1	827	5	0	0	355	-9.4	2.7	19.4	0.1
829	0	-5	10	5	-0.3	2.9	12.5	0.2	837	0	-5	50	45	-27.0	2.6	-44.2	0.2
838	0	-5	55	50	-9.3	2.5	-45.5	0.1	839	0	-5	60	55	-8.6	2.6	-51.7	0.1
840	0	-5	65	60	-25.0	2.6	-64.9	9.1	841	0	-5	70	65	-24.4	2.7	-76.7	0.2
842	0	-5	75	70	-39.9	2.6	-89.6	0.1	843	0	-5	80	75	-46.1	2.5	-96.6	0.1
844	0	-5	85	80	-42.5	2.5	-91.8	0.1	845	0	-5	90	85	-23.9	2.5	-74.0	0.1
846	0	-5	95	90	-8.5	2.6	-50.1	0.1	847	0	-5	100	95	10.5	2.6	-24.0	0.1
848	0	-5	105	100	35.2	4.0	2.1	0.6	849	0	-5	110	105	38.0	2.8	23.4	0.1
853	0	-5	130	125	15.5	2.7	60.4	0.1	854	0	-5	135	130	31.2	2.6	67.6	0.2
855	0	-5	140	135	29.0	3.4	73.1	0.5	856	0	-5	145	140	37.2	3.1	76.3	0.4
857	0	-5	150	145	44.7	2.5	75.5	0.1	858	0	-5	155	150	21.0	2.5	65.9	0.1
859	0	-5	160	155	20.1	2.5	59.6	0.1	860	0	-5	165	160	8.1	2.6	48.8	0.1
863	0	-5	180	175	-6.7	2.5	25.5	0.1	864	0	-5	185	180	-8.2	2.4	20.4	0.1
865	0	-5	190	185	-3.9	2.4	17.6	0.1	866	0	-5	195	190	-2.4	2.5	15.9	0.1
867	0	-5	200	195	3.8	2.4	13.9	0.1	868	0	-5	205	200	10.7	2.4	16.0	0.1
869	0	-5	210	205	14.7	2.5	14.8	0.1	870	0	-5	215	210	17.0	2.5	11.1	0.1
877	0	-5	250	245	-2.6	2.5	-17.6	0.1	878	0	-5	255	250	-3.2	2.5	-15.7	0.1
879	0	-5	260	255	-7.5	2.6	-14.8	0.1	880	0	-5	265	260	-6.7	2.6	-12.7	0.1
881	0	-5	270	265	-8.0	2.5	-9.4	0.1	882	0	-5	275	270	-4.4	2.5	-2.9	0.1
883	0	-5	280	275	2.2	2.9	6.0	0.2	893	0	-5	330	325	-3.7	2.5	-4.1	0.1
894	0	-5	335	330	0.4	2.5	2.2	0.1	895	0	-5	340	335	-2.5	2.5	7.4	0.1
896	0	-5	345	340	5.8	2.5	14.7	0.1	897	0	-5	350	345	11.7	2.5	20.3	0.1

SEQ	LAT		LONG		ANOM	S.D.	UND	S.D.
898	0	-5	355	350	4.3	2.5	19.7	0.1
900	-5	-10	5	0	-5.2	2.6	11.9	0.1
907	-5	-10	41	35	-9.9	5.8	-27.5	1.3
909	-5	-10	51	46	-18.6	2.5	-37.7	0.1
911	-5	-10	61	56	0.0	2.7	-42.8	0.1
913	-5	-10	71	66	-21.1	2.5	-65.9	0.1
915	-5	-10	81	76	-39.1	2.8	-83.4	0.2
917	-5	-10	91	86	-24.9	2.5	-67.0	0.1
919	-5	-10	101	96	3.4	2.5	-27.0	0.1
921	-5	-10	112	106	31.8	2.6	18.5	0.1
923	-5	-10	122	117	38.7	2.9	41.7	0.2
926	-5	-10	137	132	21.5	2.5	63.0	0.1
930	-5	-10	157	152	20.1	2.5	67.6	0.1
934	-5	-10	177	172	-5.2	2.4	37.1	0.1
936	-5	-10	188	183	-11.7	2.4	22.2	0.1
938	-5	-10	198	193	1.3	2.5	16.4	0.1
940	-5	-10	208	203	5.3	2.5	11.4	0.1
946	-5	-10	238	233	0.0	2.8	-11.7	0.1
949	-5	-10	254	248	4.6	2.6	-12.4	0.1
951	-5	-10	264	259	-8.8	2.5	-12.7	0.1
953	-5	-10	274	269	-11.1	2.6	-7.1	0.1
964	-5	-10	330	325	-10.4	2.7	-7.3	0.1
966	-5	-10	340	335	-8.4	2.7	1.8	0.1
968	-5	-10	350	345	9.1	2.5	16.0	0.1
970	-5	-10	0	355	6.6	2.5	16.0	0.1
972	-10	-15	10	5	3.1	2.8	14.1	0.2
979	-10	-15	46	41	-14.1	2.5	-25.4	0.1
981	-10	-15	57	51	-1.1	2.6	-32.5	0.1
983	-10	-15	67	62	-1.8	2.6	-39.2	0.2
985	-10	-15	77	72	-21.8	2.5	-60.7	0.1
987	-10	-15	87	82	-24.3	2.5	-65.7	0.1
989	-10	-15	98	93	-13.7	2.5	-43.3	0.1
991	-10	-15	108	103	1.2	2.5	-14.5	0.1
993	-10	-15	118	113	-14.9	2.4	9.2	0.1
995	-10	-15	129	123	27.0	2.8	47.7	0.1
998	-10	-15	144	139	21.1	3.1	65.4	0.3
1003	-10	-15	170	165	11.8	2.5	58.4	0.1
1005	-10	-15	180	175	12.2	2.5	46.8	0.1
1007	-10	-15	190	185	3.6	2.5	28.6	0.1
1009	-10	-15	201	195	0.3	2.5	16.3	0.1
1011	-10	-15	211	206	-1.0	2.6	5.4	0.1
1015	-10	-15	231	226	1.4	2.6	-8.3	0.1
1017	-10	-15	242	237	6.1	2.5	-7.7	0.1
1019	-10	-15	252	247	11.0	2.5	-4.7	0.1
1021	-10	-15	262	257	-3.0	2.5	-8.8	0.1
1023	-10	-15	273	267	-6.2	2.6	-8.0	0.1
1025	-10	-15	283	278	-16.7	2.6	8.2	0.1
1035	-10	-15	334	329	-10.5	2.5	-6.4	0.1
1037	-10	-15	345	339	-3.0	2.8	6.3	0.1
1039	-10	-15	355	350	1.1	2.4	13.0	0.1
1041	-15	-20	5	0	-0.8	2.5	15.8	0.1
1048	-15	-20	42	37	-13.7	3.0	-12.6	0.3
1050	-15	-20	52	47	14.9	3.5	-10.5	0.5
1052	-15	-20	63	57	14.0	2.7	-20.5	0.1

SEQ	LAT		LONG		ANOM	S.D.	UND	S.D.
899	0	-5	0	355	4.1	2.5	18.7	0.1
901	-5	-10	10	5	-7.1	2.8	9.6	0.2
908	-5	-10	46	41	-26.1	2.4	-35.1	0.1
910	-5	-10	56	51	-4.8	2.5	-37.7	0.1
912	-5	-10	66	61	-15.4	2.8	-54.6	0.2
914	-5	-10	76	71	-26.8	2.7	-77.0	0.1
916	-5	-10	86	81	-32.0	2.5	-79.0	0.1
918	-5	-10	96	91	-16.1	2.6	-49.7	0.1
920	-5	-10	106	101	1.7	2.7	-7.7	0.2
922	-5	-10	117	112	35.8	2.5	32.0	0.1
925	-5	-10	132	127	-23.6	2.5	47.5	0.1
929	-5	-10	152	147	29.1	2.7	72.8	0.1
931	-5	-10	162	157	16.5	2.6	62.1	0.1
935	-5	-10	183	177	-10.9	2.3	35.3	0.1
937	-5	-10	193	183	-8.0	2.4	18.3	0.1
939	-5	-10	203	198	1.4	2.4	13.5	0.1
941	-5	-10	213	208	6.2	2.5	8.4	0.1
947	-5	-10	243	238	-1.6	2.5	-13.0	0.1
950	-5	-10	259	254	-3.1	2.6	-11.6	0.1
952	-5	-10	269	264	-10.1	2.5	-11.3	0.1
954	-5	-10	279	274	-11.4	2.6	-0.2	0.1
965	-5	-10	335	330	-10.6	2.7	-4.4	0.2
967	-5	-10	345	340	4.4	2.5	10.4	0.1
969	-5	-10	355	350	3.6	2.4	16.2	0.1
971	-10	-15	5	0	-3.2	2.5	12.2	0.1
973	-10	-15	15	10	15.9	3.6	17.8	0.6
980	-10	-15	51	46	2.0	2.6	-28.8	0.1
982	-10	-15	62	57	3.3	2.6	-31.6	0.1
984	-10	-15	72	67	-4.8	2.5	-49.0	0.1
986	-10	-15	82	77	-21.0	2.5	-65.4	0.1
988	-10	-15	93	87	-30.6	2.6	-71.0	0.1
990	-10	-15	103	98	-9.2	2.5	-30.3	0.1
992	-10	-15	113	108	-1.0	2.5	-1.6	0.1
994	-10	-15	123	118	-2.2	2.6	24.2	0.1
997	-10	-15	139	134	23.7	2.9	60.4	0.3
1000	-10	-15	154	149	11.5	2.5	67.3	0.1
1004	-10	-15	175	170	22.3	2.5	55.6	0.1
1006	-10	-15	185	180	10.5	2.5	38.5	0.1
1008	-10	-15	195	190	-2.2	2.5	19.5	0.1
1010	-10	-15	206	201	-1.0	2.5	8.9	0.1
1012	-10	-15	216	211	-3.7	2.6	0.4	0.1
1016	-10	-15	237	231	2.9	2.6	-10.9	0.1
1018	-10	-15	247	242	10.8	2.6	-5.6	0.1
1020	-10	-15	257	252	6.9	2.5	-6.3	0.1
1022	-10	-15	267	262	-1.4	2.4	-8.3	0.1
1024	-10	-15	278	273	-10.0	2.5	-1.6	0.1
1034	-10	-15	329	324	-7.4	2.5	-7.9	0.1
1036	-10	-15	339	334	-10.1	2.6	-2.7	0.1
1038	-10	-15	350	345	1.5	2.5	11.2	0.1
1040	-10	-15	0	355	-1.2	2.6	12.9	0.1
1042	-15	-20	10	5	-3.9	2.4	17.7	0.1
1049	-15	-20	47	42	3.9	3.4	-12.3	0.6
1051	-15	-20	57	52	6.9	2.6	-14.3	0.2
1053	-15	-20	68	63	13.1	2.7	-21.7	0.2

SEQ	LAT		LONG		ANOM	S.D.	UND	S.D.	SEQ	LAT		LONG		ANOM	S.D.	UND	S.D.
1054	-15	-20	73	68	4.6	2.5	-31.1	0.1	1055	-15	-20	78	73	-4.7	2.5	-41.3	0.1
1056	-15	-20	83	78	-11.2	2.6	-48.6	0.1	1057	-15	-20	89	83	-18.0	2.7	-62.6	0.1
1058	-15	-20	94	89	-22.4	2.5	-51.4	0.1	1059	-15	-20	99	94	-22.6	2.5	-46.4	0.1
1060	-15	-20	104	99	-26.0	2.4	-39.0	0.1	1061	-15	-20	110	104	-25.9	2.5	-31.3	0.1
1062	-15	-20	115	110	-17.7	2.4	-12.8	0.1	1063	-15	-20	120	115	-13.4	2.7	1.4	0.1
1064	-15	-20	125	120	13.4	3.7	19.0	0.7	1069	-15	-20	151	146	18.9	2.9	61.4	0.2
1070	-15	-20	157	151	19.5	2.6	73.7	0.1	1072	-15	-20	167	162	17.9	2.5	60.4	0.1
1073	-15	-20	172	167	31.4	2.5	63.7	0.1	1074	-15	-20	177	172	32.4	2.5	61.2	0.1
1075	-15	-20	183	177	25.9	2.5	62.0	0.1	1076	-15	-20	188	183	22.5	2.5	41.6	0.1
1077	-15	-20	193	188	6.7	2.4	25.4	0.1	1078	-15	-20	198	193	-3.6	2.4	15.4	0.1
1079	-15	-20	203	198	0.5	2.5	10.2	0.1	1080	-15	-20	209	203	5.1	2.5	7.0	0.1
1081	-15	-20	214	209	4.0	2.8	1.1	0.1	1084	-15	-20	230	224	-5.3	2.5	-12.3	0.1
1085	-15	-20	235	230	0.8	2.4	-9.1	0.1	1086	-15	-20	240	235	6.5	2.5	-6.4	0.1
1087	-15	-20	245	240	11.1	2.5	-3.4	0.1	1088	-15	-20	250	245	12.7	2.5	-1.8	0.1
1089	-15	-20	256	250	11.2	2.7	-3.7	0.2	1090	-15	-20	261	256	4.0	2.5	-4.7	0.1
1091	-15	-20	266	261	2.4	2.5	-4.6	0.1	1092	-15	-20	271	266	-0.0	2.7	-3.4	0.2
1093	-15	-20	277	271	-5.0	2.6	-1.0	0.1	1094	-15	-20	282	277	-0.7	2.5	7.7	0.1
1095	-15	-20	287	282	1.0	2.7	18.0	0.2	1103	-15	-20	329	323	-2.9	2.7	-7.0	0.2
1104	-15	-20	334	329	-7.4	2.5	-5.1	0.1	1105	-15	-20	339	334	-13.3	2.7	-3.8	0.1
1106	-15	-20	344	339	-2.0	2.7	3.6	0.2	1107	-15	-20	350	344	3.5	2.5	12.1	0.1
1108	-15	-20	355	350	1.1	2.6	12.8	0.1	1110	-20	-25	5	0	5.9	2.6	21.1	0.1
1111	-20	-25	11	5	12.4	2.5	29.7	0.1	1116	-20	-25	38	32	-5.8	4.0	4.7	0.7
1117	-20	-25	43	38	-1.3	2.5	-0.6	0.1	1119	-20	-25	54	48	-4.1	2.7	-3.8	0.1
1120	-20	-25	59	54	10.1	2.6	-2.8	0.1	1121	-20	-25	64	59	12.5	2.6	-4.3	0.1
1122	-20	-25	70	64	21.4	2.6	-8.9	0.1	1123	-20	-25	75	70	11.2	2.5	-16.5	0.1
1124	-20	-25	81	75	0.0	2.5	-33.5	0.1	1125	-20	-25	86	81	-6.3	2.6	-36.2	0.2
1126	-20	-25	91	86	-7.1	2.5	-40.2	0.1	1127	-20	-25	97	91	-20.3	2.5	-53.0	0.1
1128	-20	-25	102	97	-25.8	2.4	-43.3	0.1	1129	-20	-25	107	102	-16.5	2.4	-35.9	0.1
1130	-20	-25	113	107	-22.5	2.5	-33.1	0.1	1131	-20	-25	118	113	3.0	4.3	-11.8	0.9
1138	-20	-25	156	150	18.7	2.7	62.4	0.1	1139	-20	-25	161	156	11.2	2.4	52.1	0.1
1140	-20	-25	167	161	18.4	2.5	65.9	0.1	1141	-20	-25	172	167	17.7	2.4	56.8	0.1
1142	-20	-25	177	172	24.4	2.5	56.5	0.1	1143	-20	-25	183	177	28.7	2.5	62.0	0.1
1144	-20	-25	188	183	11.3	2.4	38.6	0.1	1145	-20	-25	193	188	5.1	2.4	25.1	0.1
1146	-20	-25	199	193	-1.5	2.5	16.9	0.1	1147	-20	-25	204	199	6.2	2.5	9.1	0.1
1148	-20	-25	210	204	-2.1	2.5	2.1	0.1	1149	-20	-25	215	210	-7.3	2.5	-4.3	0.1
1151	-20	-25	226	220	-6.7	2.5	-12.5	0.1	1152	-20	-25	231	226	-4.2	2.4	-11.0	0.1
1153	-20	-25	236	231	-1.9	2.4	-9.6	0.1	1154	-20	-25	242	236	4.5	2.5	-7.4	0.1
1155	-20	-25	247	242	6.8	2.5	-3.4	0.1	1156	-20	-25	253	247	8.5	2.6	-2.9	0.1
1157	-20	-25	258	253	2.3	2.6	-3.0	0.1	1158	-20	-25	263	258	4.0	2.5	-2.2	0.1
1159	-20	-25	269	263	8.2	2.8	-0.5	0.2	1160	-20	-25	274	269	5.2	2.5	1.9	0.1
1161	-20	-25	279	274	3.2	2.5	5.4	0.1	1162	-20	-25	285	279	-1.3	2.6	14.8	0.1
1163	-20	-25	290	285	-6.8	2.8	21.1	0.1	1171	-20	-25	333	328	-10.2	2.5	-4.4	0.1
1172	-20	-25	339	333	-14.1	2.6	-2.2	0.1	1173	-20	-25	344	339	-6.2	2.5	4.2	0.1
1174	-20	-25	349	344	4.5	2.4	10.8	0.1	1175	-20	-25	355	349	-0.4	2.8	15.7	0.3
1176	-20	-25	0	355	0.6	2.7	16.7	0.2	1177	-25	-30	6	0	11.1	2.5	24.5	0.1
1178	-25	-30	11	6	5.0	2.5	21.7	0.1	1179	-25	-30	17	11	16.5	3.3	30.8	0.5
1182	-25	-30	34	28	20.3	5.2	24.0	1.1	1183	-25	-30	39	34	0.1	2.5	11.5	0.1
1184	-25	-30	45	39	-7.6	2.5	9.7	0.1	1185	-25	-30	51	45	5.7	2.5	10.6	0.1
1186	-25	-30	56	51	-1.4	2.4	5.9	0.1	1187	-25	-30	62	56	3.0	2.5	6.9	0.1
1188	-25	-30	68	62	16.2	2.5	6.3	0.1	1189	-25	-30	73	68	18.9	2.4	0.9	0.1
1190	-25	-30	79	73	10.2	2.5	-8.0	0.1	1191	-25	-30	84	79	2.9	2.5	-14.9	0.1
1192	-25	-30	90	84	-0.8	2.5	-26.3	0.1	1193	-25	-30	96	90	-18.6	2.5	-35.2	0.1
1194	-25	-30	101	96	-10.0	2.4	-31.2	0.1	1195	-25	-30	107	101	-11.5	2.5	-37.2	0.1
1196	-25	-30	113	107	-24.0	2.5	-34.1	0.1	1197	-25	-30	118	113	3.9	5.2	-17.4	1.1

SEQ	LAT		LONG		ANOM	S.D.	UND	S.D.	SEQ	LAT		LONG		ANOM	S.D.	UND	S.D.
1204	-25	-30	158	152	7.9	2.8	39.5	0.2	1205	-25	-30	163	158	9.2	2.4	35.1	0.1
1206	-25	-30	169	163	10.1	2.5	45.6	0.1	1207	-25	-30	174	169	18.8	2.4	41.8	0.1
1208	-25	-30	180	174	18.0	2.5	48.7	0.1	1209	-25	-30	186	180	17.1	2.5	40.2	0.1
1210	-25	-30	191	186	17.8	2.4	24.5	0.1	1211	-25	-30	197	191	0.6	2.5	16.6	0.1
1212	-25	-30	203	197	-0.7	2.5	8.0	0.1	1213	-25	-30	208	203	-2.7	2.5	1.7	0.1
1214	-25	-30	214	208	0.8	2.6	-2.4	0.1	1216	-25	-30	225	219	-6.6	2.5	-10.6	0.1
1217	-25	-30	231	225	-8.4	2.5	-12.4	0.1	1218	-25	-30	236	231	-3.4	2.4	-9.1	0.1
1219	-25	-30	242	236	-1.6	2.5	-8.6	0.1	1220	-25	-30	248	242	-0.8	2.8	-6.4	0.3
1221	-25	-30	253	248	-1.5	2.5	-4.7	0.1	1222	-25	-30	259	253	1.7	2.6	-3.5	0.1
1223	-25	-30	264	259	2.0	2.6	-1.6	0.1	1224	-25	-30	270	264	5.6	2.5	0.8	0.1
1225	-25	-30	276	270	5.2	2.6	3.7	0.1	1226	-25	-30	281	276	3.2	2.5	7.0	0.1
1227	-25	-30	287	281	10.6	2.5	15.3	0.1	1228	-25	-30	293	287	34.8	4.9	30.9	1.0
1232	-25	-30	315	309	-2.1	3.2	-0.1	0.4	1234	-25	-30	326	321	-8.5	2.9	-4.1	0.3
1235	-25	-30	332	326	-1.2	2.7	-0.1	0.1	1236	-25	-30	338	332	-0.1	2.7	3.8	0.1
1237	-25	-30	343	338	1.6	2.5	7.3	0.1	1238	-25	-30	349	343	6.0	2.7	12.7	0.2
1239	-25	-30	354	349	3.8	2.9	12.9	0.2	1240	-25	-30	0	354	4.5	2.9	18.9	0.3
1241	-30	-35	6	0	3.7	2.5	22.6	0.1	1242	-30	-35	12	6	2.2	2.5	25.3	0.1
1243	-30	-35	18	12	6.1	2.8	29.4	0.1	1245	-30	-35	30	24	17.7	4.7	31.6	1.0
1246	-30	-35	35	30	5.5	2.5	22.9	0.1	1247	-30	-35	41	35	0.4	2.5	22.5	0.1
1248	-30	-35	47	41	22.6	2.5	26.3	0.1	1249	-30	-35	53	47	7.1	2.5	23.5	0.1
1250	-30	-35	59	53	19.8	2.5	22.5	0.1	1251	-30	-35	65	59	12.5	2.6	18.2	0.1
1252	-30	-35	71	65	14.4	2.5	13.7	0.1	1254	-30	-35	83	77	11.6	2.5	-1.8	0.1
1255	-30	-35	89	83	6.6	2.5	-12.0	0.1	1256	-30	-35	94	89	-3.0	2.4	-18.3	0.1
1257	-30	-35	100	94	-10.8	2.5	-30.4	0.1	1258	-30	-35	106	100	-23.9	2.5	-37.4	0.1
1259	-30	-35	112	106	-21.3	2.5	-38.1	0.1	1260	-30	-35	118	112	-15.8	3.0	-32.1	0.5
1262	-30	-35	130	124	-17.7	3.5	-21.2	0.6	1263	-30	-35	136	130	-11.3	3.5	-10.9	0.6
1267	-30	-35	159	153	-7.3	2.5	24.7	0.1	1268	-30	-35	165	159	3.4	2.5	30.6	0.1
1269	-30	-35	171	165	11.0	2.5	36.4	0.1	1270	-30	-35	177	171	23.8	2.5	41.9	0.1
1271	-30	-35	183	177	17.9	2.4	37.3	0.1	1272	-30	-35	189	183	15.2	2.4	26.9	0.1
1273	-30	-35	195	189	1.7	2.5	17.3	0.1	1274	-30	-35	201	195	4.1	2.5	9.4	0.1
1275	-30	-35	207	201	2.1	2.5	2.8	0.1	1276	-30	-35	212	207	2.2	3.1	-1.6	0.3
1278	-30	-35	224	218	-2.3	2.6	-9.7	0.1	1279	-30	-35	230	224	-4.2	2.5	-11.5	0.1
1280	-30	-35	236	230	-1.6	2.5	-10.9	0.1	1281	-30	-35	242	236	-3.2	2.5	-10.3	0.1
1282	-30	-35	248	242	-5.0	2.5	-9.5	0.1	1283	-30	-35	254	248	-5.9	2.5	-8.1	0.1
1284	-30	-35	260	254	-4.0	2.7	-5.9	0.2	1285	-30	-35	266	260	-5.3	2.6	-3.9	0.1
1286	-30	-35	271	266	-0.5	2.4	-0.7	0.1	1287	-30	-35	277	271	-2.9	2.5	1.9	0.1
1288	-30	-35	283	277	0.5	2.5	8.4	0.1	1289	-30	-35	289	283	-5.2	2.8	15.4	0.1
1293	-30	-35	313	307	1.9	2.7	3.8	0.1	1294	-30	-35	319	313	-15.0	2.5	-5.7	0.1
1295	-30	-35	325	319	-8.7	2.5	-4.0	0.1	1296	-30	-35	330	325	4.4	2.5	3.0	0.1
1297	-30	-35	336	330	6.3	2.6	8.4	0.1	1298	-30	-35	342	336	7.7	2.6	13.1	0.1
1301	-30	-35	0	354	2.9	2.8	19.1	0.1	1302	-35	-40	6	0	-5.7	2.5	19.9	0.1
1303	-35	-40	13	6	-1.4	2.5	28.5	0.1	1304	-35	-40	19	13	-0.4	2.5	28.1	0.1
1305	-35	-40	25	19	1.9	3.4	30.8	0.5	1306	-35	-40	32	25	7.5	2.5	37.2	0.1
1307	-35	-40	38	32	5.5	2.5	31.7	0.1	1308	-35	-40	44	38	11.4	2.5	34.1	0.1
1309	-35	-40	51	44	34.0	2.5	44.8	0.1	1310	-35	-40	57	51	21.0	2.6	33.9	0.1
1311	-35	-40	63	57	6.5	3.5	26.6	0.5	1312	-35	-40	69	63	16.7	3.2	23.8	0.5
1313	-35	-40	76	69	13.4	3.2	19.8	0.5	1314	-35	-40	82	76	16.1	3.3	10.7	0.5
1315	-35	-40	88	82	7.4	3.2	0.6	0.5	1316	-35	-40	95	88	1.8	2.5	-12.6	0.1
1317	-35	-40	101	95	-8.7	2.5	-22.7	0.1	1318	-35	-40	107	101	-16.2	2.4	-31.3	0.1
1319	-35	-40	114	107	-27.9	3.2	-41.1	0.5	1320	-35	-40	120	114	-29.8	3.4	-35.3	0.3
1321	-35	-40	126	120	-32.3	2.7	-33.3	0.1	1322	-35	-40	133	126	-34.7	2.6	-32.1	0.1
1323	-35	-40	139	133	-22.2	2.6	-15.7	0.1	1324	-35	-40	145	139	1.7	4.4	0.1	0.9
1325	-35	-40	152	145	3.6	3.6	10.4	0.6	1326	-35	-40	158	152	-4.1	2.4	10.1	0.1
1327	-35	-40	164	158	-7.8	2.4	14.5	0.1	1328	-35	-40	171	164	15.1	2.5	27.4	0.1

SEQ	LAT		LONG		ANOM	S.D.	UND	S.D.
1329	-35	-40	177	171	24.4	2.7	29.2	0.2
1331	-35	-40	189	183	8.9	2.5	18.6	0.1
1333	-35	-40	202	196	8.1	2.5	5.6	0.1
1337	-35	-40	227	221	-1.1	2.5	-11.3	0.1
1339	-35	-40	240	234	-2.6	2.5	-11.6	0.1
1341	-35	-40	253	246	-5.8	2.6	-11.2	0.1
1343	-35	-40	265	259	-1.5	2.5	-4.8	0.1
1345	-35	-40	278	272	-3.9	2.4	1.8	0.1
1347	-35	-40	291	284	22.0	4.4	23.7	0.9
1351	-35	-40	316	309	-16.6	2.5	-3.5	0.1
1353	-35	-40	328	322	-10.3	2.6	-0.9	0.1
1355	-35	-40	341	335	15.0	3.9	17.7	0.3
1359	-40	-45	7	0	-6.1	3.0	21.3	0.2
1361	-40	-45	20	14	4.3	2.5	25.7	0.1
1363	-40	-45	34	27	1.3	2.5	35.0	0.1
1365	-40	-45	48	41	21.7	2.5	43.9	0.1
1367	-40	-45	61	54	14.0	2.5	36.0	0.1
1369	-40	-45	75	68	14.6	2.6	23.9	0.1
1371	-40	-45	88	82	12.4	2.5	9.6	0.1
1373	-40	-45	102	95	0.3	2.3	-12.0	0.1
1375	-40	-45	115	109	-13.4	2.5	-24.8	0.1
1377	-40	-45	129	122	-13.6	2.5	-27.8	0.1
1379	-40	-45	143	136	-16.4	2.5	-15.7	0.1
1381	-40	-45	156	149	-14.7	2.5	-4.3	0.1
1383	-40	-45	170	163	-2.9	2.6	7.5	0.1
1385	-40	-45	183	177	21.7	2.3	12.6	0.1
1387	-40	-45	197	190	0.1	2.5	0.5	0.1
1392	-40	-45	231	224	-2.8	2.5	-13.5	0.1
1394	-40	-45	245	238	-2.1	2.5	-11.4	0.1
1396	-40	-45	258	251	-2.3	2.5	-3.6	0.1
1398	-40	-45	272	265	1.7	2.5	-1.8	0.1
1400	-40	-45	285	278	2.7	2.5	9.6	0.1
1403	-40	-45	306	299	-2.9	2.5	7.3	0.1
1405	-40	-45	319	312	-15.4	2.5	-4.3	0.1
1407	-40	-45	333	326	-3.0	2.5	6.6	0.1
1411	-40	-45	0	353	2.5	2.9	22.3	0.2
1414	-45	-50	22	15	2.9	3.3	31.8	0.5
1416	-45	-50	37	29	21.6	2.5	47.3	0.1
1418	-45	-50	51	44	20.3	2.5	43.5	0.1
1420	-45	-50	66	59	9.3	2.5	36.2	0.1
1422	-45	-50	81	73	22.1	2.5	32.0	0.1
1424	-45	-50	96	88	15.1	2.5	3.8	0.1
1426	-45	-50	110	103	0.0	2.5	-14.6	0.1
1429	-45	-50	132	125	-4.7	2.4	-23.0	0.1
1431	-45	-50	147	140	-7.0	2.5	-15.5	0.1
1433	-45	-50	162	154	-10.9	2.5	-12.0	0.1
1435	-45	-50	176	169	3.1	2.5	-2.0	0.1
1437	-45	-50	191	184	-10.0	2.5	-10.3	0.1
1439	-45	-50	206	198	2.1	2.3	-12.8	0.1
1443	-45	-50	235	228	0.8	2.5	-13.6	0.1
1445	-45	-50	250	242	5.9	2.6	-10.9	0.1
1447	-45	-50	264	257	0.3	2.5	-7.5	0.1
1449	-45	-50	279	272	2.1	2.4	2.7	0.1
1452	-45	-50	301	294	1.9	2.5	11.6	0.1

SEQ	LAT		LONG		ANOM	S.D.	UND	S.D.
1330	-35	-40	183	177	3.4	2.5	23.9	0.1
1332	-35	-40	196	189	8.4	2.5	13.3	0.1
1334	-35	-40	208	202	4.8	2.7	0.2	0.1
1338	-35	-40	234	227	-1.1	2.5	-13.5	0.1
1340	-35	-40	246	240	-3.9	2.5	-11.2	0.1
1342	-35	-40	259	253	-4.9	2.3	-7.7	0.1
1344	-35	-40	272	265	-1.1	2.5	-2.5	0.1
1346	-35	-40	284	278	3.9	2.5	9.0	0.1
1350	-35	-40	309	303	4.6	2.6	7.7	0.1
1352	-35	-40	322	316	-14.7	2.5	-5.4	0.1
1354	-35	-40	335	328	3.3	2.5	11.1	0.1
1358	-35	-40	0	354	-6.7	2.9	18.4	0.2
1360	-40	-45	14	7	4.7	2.7	26.6	0.2
1362	-40	-45	27	20	8.3	2.7	33.8	0.1
1364	-40	-45	41	34	22.8	2.5	41.6	0.1
1366	-40	-45	54	48	14.7	2.4	35.8	0.1
1368	-40	-45	68	61	9.2	2.6	30.0	0.1
1370	-40	-45	82	75	16.6	2.5	19.7	0.1
1372	-40	-45	95	88	11.7	2.5	0.9	0.1
1374	-40	-45	109	102	-3.1	2.5	-22.7	0.1
1376	-40	-45	122	115	-13.4	2.7	-29.8	0.1
1378	-40	-45	136	129	-13.5	2.5	-22.7	0.1
1380	-40	-45	149	143	4.3	2.5	-5.0	0.2
1382	-40	-45	163	156	-9.3	2.5	0.2	0.1
1384	-40	-45	177	170	12.4	2.6	13.2	0.1
1386	-40	-45	190	183	9.5	2.5	7.3	0.1
1388	-40	-45	204	197	3.9	2.5	-2.5	0.1
1393	-40	-45	238	231	1.3	2.5	-11.9	0.1
1395	-40	-45	251	245	-1.8	2.5	-8.8	0.1
1397	-40	-45	265	258	-0.5	2.5	-5.7	0.1
1399	-40	-45	278	273	4.0	2.4	3.1	0.1
1402	-40	-45	299	292	2.2	3.3	14.2	0.5
1404	-40	-45	312	306	-10.5	2.4	-0.7	0.1
1406	-40	-45	326	319	-17.1	2.5	-3.3	0.1
1408	-40	-45	340	333	12.5	2.9	17.9	0.2
1413	-45	-50	15	7	-3.9	3.0	30.4	0.2
1415	-45	-50	29	22	1.5	2.6	34.5	0.1
1417	-45	-50	44	37	13.7	2.5	44.5	0.1
1419	-45	-50	59	51	23.6	2.5	49.2	0.1
1421	-45	-50	73	66	30.3	2.6	35.8	0.1
1423	-45	-50	88	81	18.3	2.5	19.0	0.1
1425	-45	-50	103	96	6.9	2.4	-4.4	0.1
1427	-45	-50	118	110	-7.1	2.5	-25.2	0.1
1430	-45	-50	140	132	-1.3	2.5	-21.4	0.1
1432	-45	-50	154	147	-7.8	2.5	-13.1	0.1
1434	-45	-50	169	162	3.9	2.5	-4.5	0.1
1436	-45	-50	184	176	-0.7	2.5	-5.8	0.1
1438	-45	-50	198	191	-4.5	2.5	-11.6	0.1
1440	-45	-50	213	206	3.9	2.8	-12.0	0.2
1444	-45	-50	242	235	5.0	2.6	-11.0	0.1
1446	-45	-50	257	250	-0.7	2.7	-9.3	0.1
1448	-45	-50	272	264	1.3	2.5	-4.1	0.1
1450	-45	-50	287	279	9.3	2.9	12.5	0.3
1453	-45	-50	309	301	-18.2	2.3	3.9	0.1

SEQ	LAT		LONG		ANOM	S.D.	UND	S.D.	SEQ	LAT		LONG		ANOM	S.D.	UND	S.D.
1454	-45	-50	316	309	-23.2	2.5	-1.8	0.1	1455	-45	-50	323	316	-17.6	2.4	-0.7	0.1
1456	-45	-50	331	323	-16.0	2.5	5.1	0.1	1457	-45	-50	338	331	2.9	2.5	14.9	0.1
1458	-45	-50	345	338	15.8	2.6	23.2	0.1	1459	-45	-50	353	345	15.2	2.7	29.9	0.1
1460	-45	-50	0	353	5.7	3.9	24.6	0.6	1464	-50	-55	33	25	9.6	2.6	37.2	0.1
1465	-50	-55	41	33	20.5	2.5	43.1	0.1	1466	-50	-55	49	41	28.0	2.5	46.3	0.1
1467	-50	-55	57	49	17.4	2.5	42.6	0.1	1468	-50	-55	65	57	7.8	2.5	37.3	0.1
1469	-50	-55	74	65	21.8	2.6	40.3	0.1	1470	-50	-55	82	74	26.5	2.5	30.5	0.1
1471	-50	-55	90	82	14.4	2.5	18.6	0.1	1472	-50	-55	98	90	11.3	2.5	7.9	0.1
1473	-50	-55	106	98	7.2	2.5	-3.2	0.1	1474	-50	-55	115	106	0.1	2.5	-15.6	0.1
1475	-50	-55	123	115	-3.1	2.9	-20.9	0.1	1476	-50	-55	131	123	-5.0	2.5	-23.1	0.1
1477	-50	-55	139	131	-0.4	2.5	-21.3	0.1	1478	-50	-55	147	139	2.3	2.5	-18.9	0.1
1479	-50	-55	155	147	-3.4	2.5	-18.9	0.1	1480	-50	-55	164	155	-1.1	2.5	-20.3	0.1
1481	-50	-55	172	164	6.5	2.5	-16.9	0.1	1482	-50	-55	180	172	-14.5	2.5	-22.4	0.1
1483	-50	-55	188	180	-16.0	2.5	-25.2	0.1	1484	-50	-55	196	188	-10.2	2.5	-24.0	0.1
1485	-50	-55	205	196	-5.1	2.6	-24.2	0.1	1486	-50	-55	213	205	-2.9	3.0	-19.4	0.2
1493	-50	-55	270	262	-1.2	2.5	-7.2	0.1	1494	-50	-55	278	270	-1.1	2.5	-1.6	0.1
1495	-50	-55	286	278	-0.2	2.7	6.2	0.1	1496	-50	-55	295	286	11.9	3.1	14.2	0.3
1497	-50	-55	303	295	8.0	2.4	13.0	0.1	1498	-50	-55	311	303	-6.9	2.5	8.6	0.1
1499	-50	-55	319	311	-1.4	2.5	7.9	0.1	1500	-50	-55	327	319	-0.2	2.5	10.4	0.1
1501	-50	-55	335	327	-1.7	2.5	13.7	0.1	1502	-50	-55	344	335	11.4	2.5	23.3	0.1
1503	-50	-55	352	344	12.9	2.8	25.2	0.1	1507	-55	-60	28	18	1.6	3.0	32.2	0.3
1508	-55	-60	37	28	6.3	2.5	33.8	0.1	1509	-55	-60	46	37	12.5	2.6	38.6	0.1
1510	-55	-60	55	46	8.3	2.5	37.4	0.1	1511	-55	-60	65	55	9.8	2.5	38.9	0.1
1512	-55	-60	74	65	15.0	2.5	32.4	0.1	1513	-55	-60	83	74	21.4	2.4	27.1	0.1
1514	-55	-60	92	83	6.7	2.5	14.6	0.1	1515	-55	-60	102	93	8.0	2.5	3.3	0.1
1516	-55	-60	111	102	1.9	2.5	-8.6	0.1	1517	-55	-60	120	111	-4.9	2.9	-18.7	0.1
1518	-55	-60	129	120	-10.5	3.1	-25.6	0.4	1520	-55	-60	148	138	-0.2	2.6	-29.2	0.1
1521	-55	-60	157	148	1.7	2.5	-26.3	0.1	1522	-55	-60	166	157	-20.2	2.5	-32.1	0.1
1523	-55	-60	175	166	-29.8	2.5	-38.3	0.1	1524	-55	-60	185	175	-30.1	2.7	-44.7	0.2
1525	-55	-60	194	185	-22.0	2.8	-38.3	0.2	1526	-55	-60	203	194	-10.0	2.7	-32.8	0.1
1527	-55	-60	212	203	-5.8	3.1	-28.8	0.2	1532	-55	-60	258	249	-0.6	4.3	-15.7	0.9
1533	-55	-60	268	258	-2.1	2.5	-13.4	0.1	1534	-55	-60	277	268	-2.6	2.4	-6.3	0.1
1535	-55	-60	286	277	-0.3	2.4	1.4	0.1	1536	-55	-60	295	286	11.0	2.5	11.6	0.1
1537	-55	-60	305	295	24.5	2.3	20.1	0.1	1538	-55	-60	314	303	17.6	2.5	18.5	0.1
1539	-55	-60	323	314	9.8	2.4	18.3	0.1	1540	-55	-60	332	323	30.0	2.5	21.0	0.1
1541	-55	-60	342	332	-2.5	2.5	19.2	0.1	1542	-55	-60	351	342	7.7	2.7	20.9	0.1
1546	-60	-65	33	22	-2.2	2.9	24.7	0.2	1547	-60	-65	44	33	6.4	2.6	29.9	0.1
1548	-60	-65	55	44	2.7	2.6	31.2	0.1	1549	-60	-65	65	55	7.3	2.5	27.6	0.1
1550	-60	-65	76	65	8.7	2.6	26.2	0.1	1551	-60	-65	87	76	12.6	2.6	18.8	0.1
1552	-60	-65	98	87	-1.4	2.7	4.9	0.1	1553	-60	-65	109	98	-6.6	2.7	-8.2	0.1
1557	-60	-65	153	142	-15.7	5.3	-37.8	1.1	1558	-60	-65	164	153	-5.1	3.9	-38.0	0.6
1559	-60	-65	175	164	-18.3	3.1	-44.7	0.3	1560	-60	-65	185	175	-22.9	3.1	-44.5	0.2
1561	-60	-65	196	185	-15.4	3.2	-46.2	0.2	1567	-60	-65	262	251	-9.1	2.8	-21.3	0.2
1568	-60	-65	273	262	-8.3	2.6	-14.7	0.1	1569	-60	-65	284	273	-6.6	2.6	-5.8	0.1
1570	-60	-65	295	284	9.7	2.6	7.9	0.1	1571	-60	-65	305	295	28.3	2.8	17.4	0.1
1573	-60	-65	327	316	11.6	2.7	17.9	0.1	1574	-60	-65	338	327	8.5	2.6	16.1	0.1
1575	-60	-65	349	338	-2.2	2.7	13.5	0.1									